# Melem- and melamine-derived iminophosphoranes†

Tatyana Saplinova,[a] Christian Lehnert,[b] Uwe Böhme,[a] Jörg Wagler[a] and
Edwin Kroke*[a]

Iminophosphorane derivatives of s-triazine and tri-s-triazine, $C_3N_3(N=PCl_3)_3$ (1),
$[H_2C_3N_3NH_2(N=PPh_3)_2]Br_2$ (2), $[HC_3N_3NH_2(N=PPh_3)_2]Br$ (3), $C_6N_7(N=PCl_3)_3$ (5),
$[HC_6N_7(N=PCl_3)_3]Cl$ (6) were obtained by the Kirsanov reaction of melamine (1–3) and melem
(5 and 6) with halogenated phosphorus compounds. The products were characterized by FTIR
and solution NMR spectroscopy as well as by single-crystal X-ray diffraction. Additionally,
in order to investigate the electron density distribution in the s-triazine or s-heptazine systems
combined with the phosphinimine group, and to understand the influence of protonation on the
triazine and heptazine moieties, quantum chemical analyses of compounds 2, 3, 5 and 6 were
performed. Furthermore, by reaction of 5 with phenol the compound $C_6N_7(N=P(OPh)_3)_3$ (7) was
obtained. Its potential application as a flame retardant was examined by the UL 94
flammability test.

## Introduction

In modern chemical and material science the s-triazine and
tri-s-triazine[1] (Scheme 1) structural motifs have become more
and more important key building blocks for setting up
2-dimensional $CN_x$ networks or as precursors for $C_3N_4$-phases,
which are predicted to have an extremely high hardness,
chemical inertness and biocompatibility.[2] Especially within
the last decade numerous reports addressing industrial and
scientific application of the s-triazine and s-heptazine systems
have appeared.[3,4] Probably one of the most intriguing potential
industrial applications of s-triazine and s-heptazine derivatives
is their use as key components of halogen-free fire retardants
in cotton, resins and plastics.[5,6]

Those systems where the conjugated C–N system of triazines is
combined with phosphorus are of particular interest. Elemental
phosphorus as well as phosphorus compounds are already in
use as flame retardants and a synergistic effect has been
reported for a combination of nitrogen and phosphorus.[7]
Such compositions do not provide negative environmental
influence (as halogenated fire retardants do), and have therefore
been the subject of numerous patent applications.[8]

The synthesis of iminophosphoranes[9] proved a convenient
strategy to combine the s-triazine or s-heptazine system with a
phosphorus-containing functional group. Since the discovery
of iminophosphoranes (Scheme 2) – which are also known
as iminophosphines, phosphinimides, (mono-)phosphazenes,
phosphonium azaylides or $\lambda^5$-phosphazenes – by Staudinger
and Meyer in 1919,[10] two general synthetic routes for their
preparation have been established: (a) the Staudinger reaction,
which involves condensation of tertiary phosphines with
organoazides under elimination of a dinitrogen molecule,[10]
and (b) the Kirsanov reaction of phosphorus(v)-halides of the
type $R_nPX_{5-n}$ and an amine (Scheme 3).[11]

In general, both of these approaches can serve for the
synthesis of s-triazine and s-heptazine-based phosphinimines.

The Staudinger reaction was successfully applied to synthesize
phosphinimino-s-triazines as early as 1923.[12] Surprisingly, only
some years ago the 2,4,6-tris(triphenylphosphinimino)-s-triazine
and its derivatives 2,4-bis(triphenylphosphinimino)tetrazolo-
s-triazine and 2-triphenylphosphinimino-4-azidotetrazolo-
s-triazine were isolated and characterized by crystal structure
analysis.[13] In contrast to the triazines, the phosphinimino
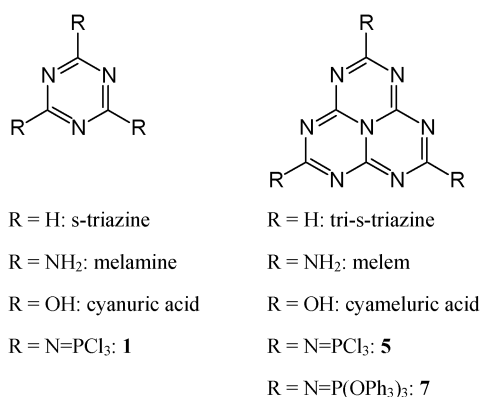


Scheme 1 s-Triazine and s-heptazine structural motifs and some of
their derivatives.

For the s-triazine derivatives:
R = H: s-triazine
R = NH₂: melamine
R = OH: cyanuric acid
R = N=PCl₃: 1

For the tri-s-triazine derivatives:
R = H: tri-s-triazine
R = NH₂: melem
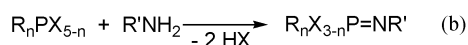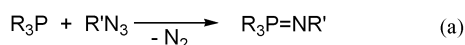R = OH: cyameluric acid
R = N=PCl₃: 5
R = N=P(OPh₃)₃: 7

[a] Institut für Anorganische Chemie, TU Bergakademie Freiberg,
Leipziger Str. 29, 09596 Freiberg, Germany.
E-mail: kroke@chemie.tu-freiberg.de; Fax: + 49 3731 39 4058;
Tel: + 49 3731 39 3174
[b] ALD Vacuum Technologies GmbH, Wilhelm-Rohn-Str. 35,
63450 Hanau, Germany.
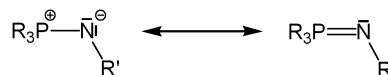
Scheme 2 General structure of the iminophosphoranes.

**Scheme 3** Staudinger (a) and Kirsanov (b) reactions. R = alkyl, aryl; X = Cl, Br, $n \leq 3$.

derivatives of s-heptazine are significantly less investigated. Several examples of 2,5,8-tris(phosphinimino)-s-heptazine were reported by our group in 2006.[8f,14] The compounds of the type $C_6N_7(N=PR_3)_3$, where R = methyl, ethyl, i-propyl, n-butyl, phenyl, m-cresyl, were prepared from cyameluric azide and the respective triorgano-phosphine. Both the explosive character of the starting materials (cyanuric[15] and cyameluric[14b,16] azides) and their tedious synthesis have to be pointed out as reasons that the Staudinger approach is inconvenient for large-scale syntheses of triazine- and heptazine-based iminophosphoranes. Hence, the Kirsanov reaction offers an alternative approach to the phosphinimino derivatives of s-triazine and s-heptazine. Melamine (2,4,6-triamino-s-triazine) and melem (2,5,8-triamino-s-heptazine) (Scheme 1), both easily available and chemically stable compounds, comprise three amino-groups in their structure, which make them advantageous starting materials for the Kirsanov reaction.

In this work we report the synthesis of s-triazine and s-heptazine-based phosphinimines by the Kirsanov reaction and their potential application as flame retardants. Furthermore, computational investigations of electronic structures of the obtained phosphinimino-s-triazines and phosphinimino-s-heptazines were performed.
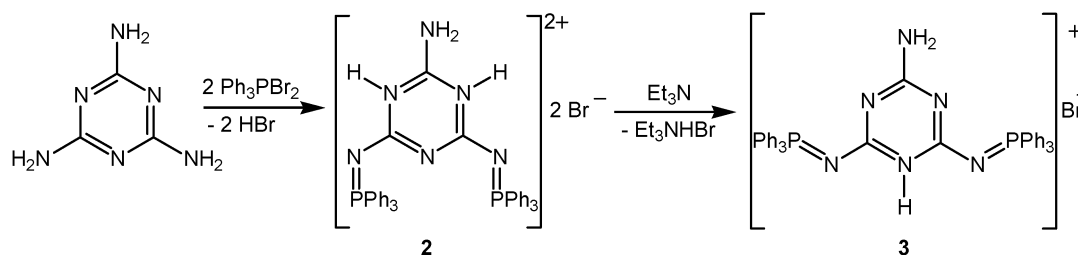
## Results and discussion

### Triazine-based iminophosphoranes

The first examples of triazine-based phosphonium salts and iminophosphoranes (compounds of the type $\{[C_3N_3(NH–PR_3)_3]^{3+} \ 3Cl^-\}$ and $C_3N_3(N=PR_3)_3$ with
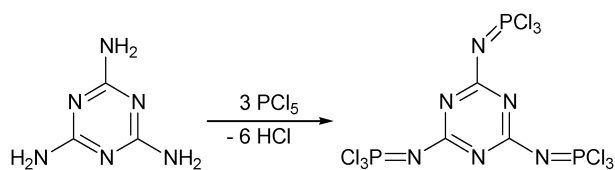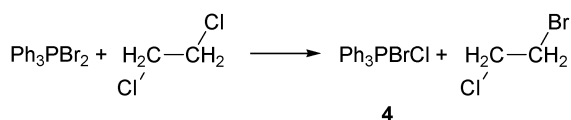
R = Cl, alkyl, aryl) synthesized by the Kirsanov reaction were reported in 1969.[17] Melamine and halogenated phosphines were engaged as the starting materials. Since then, the Kirsanov reaction remains the prevalent way to prepare phosphorus-containing triazines.[18] Among the first attempts to produce triazine-based iminophosphoranes was the reaction between melamine and phosphorus pentachloride, which leads to formation of tris(trichlorophosphinimino)triazine $C_3N_3(N=PCl_3)_3$ **1**, (Scheme 4).[18c,19]

**Synthesis and spectroscopic characterisation.** In order to compare the reactivity of melamine and melem, we reproduced the synthesis of **1**, modifying the reaction conditions (see Experimental Section and Scheme 4). Compound **1** was isolated as a white powder, well soluble in polar organic solvents. In the presence of trace amounts of water hydrolysis takes place, resulting in P=N bond splitting and formation of melamine and POCl$_3$.

One of the common reagents for the Kirsanov reaction is Ph$_3$PBr$_2$, which can be easily prepared by reacting PPh$_3$ with Br$_2$ in 1,2-dichloroethane.[20] Reflux of Ph$_3$PBr$_2$ with melamine in a 3 : 1 ratio in o-dichlorobenzene resulted in the condensation of two amino-groups of melamine with Ph$_3$PBr$_2$, thus generating two P=N bonds and liberating HBr, which in turn protonated two triazine nitrogen atoms, forming the ionic species **2** (Scheme 5). Furthermore, in an attempt to obtain neutral 2-amino-4,6-bis(triphenylphosphinimino)-s-triazine, compound **2** was treated with an excess of triethylamine in o-dichlorobenzene. The deprotonation was not complete, yielding mono-hydrobromide **3** instead of the expected product (Scheme 5).

Unfortunately, we did not succeed in further derivatisation of **2** and **3** towards the tris(triphenylphosphinimino) derivative. Changing the solvent (from o-dichlorobenzene to 1,2-dichloroethane) did not improve the synthesis: upon prolonged reflux of **2** with an excess of Ph$_3$PBr$_2$ in dichloroethane, triphenylphosphine chloride–bromide Ph$_3$PBrCl **4** (Scheme 6) was isolated. The phosphine chloride–bromide **4** is formed by exchange of the chlorine atoms of 1,2-dichloroethane with triphenylphosphine dibromide.

Similar halide-exchange reactions were reported for the complex species $[(\eta^5\text{-}C_5Me_5)RhBr]_2(\mu\text{-Br})_2$, whereby the compound $[(\eta^5\text{-}C_5Me_5)RhCl_{0.67}Br_{0.33}]_2(\mu\text{-}Cl_{0.95}Br_{0.05})_2$ was formed by recrystallisation from 1,2-dichloroethane,[21] and for α,α′-dibromo-o-xylene, which in 1,2-dichloroethane in the presence of bis(N,N-diethyldithiocarbamato)nickel(II) formed the α,α′-dichloro-o-xylene and the α,α′-bromochloro-o-xylene.[22]

**Scheme 4** Synthesis of tris(trichlorophosphinimino)-s-triazine **1**.

**Scheme 5** The Kirsanov reaction between melamine and triphenylphosphine dibromide and subsequent deprotonation of the obtained compound **2**.

**Scheme 6** Anion-exchange reaction between triphenylphosphine dibromide and 1,2-dichloroethane.

Compounds **2**, 2-amino-4,6-bis(triphenylphosphinimino)-s-triazine dihydrobromide [$H_2NH_2C_3N_3(N{=}PPh_3)_2$]$Br_2$ and **3**, 2-amino-4,6-bis(triphenylphosphinimino)-s-triazine hydrobromide [$HNH_2C_3N_3(N{=}PPh_3)_2$]$Br$, were isolated as white solids, which proved soluble in polar organic solvents.

The isolated substances **1–3** were characterized by means of FTIR- and NMR-spectroscopy and single-crystal XRD analyses. The triazine-core stretching vibrations of **1** appear as three signals at 1580, 1460 and 1250 cm$^{-1}$ (the spectrum is not shown here). In case of **2** and **3** these bands were found at 1615, 1520, 1320 and 1640, 1550, 1290 cm$^{-1}$, respectively (Fig. 1). The P$=$N valence vibrations of these compounds appear at 1410 (**1**), 1390 (**2**) and 1330 (**3**) cm$^{-1}$. Compared with corresponding data reported for other iminophosphoranes (1140–1370 cm$^{-1}$),[9] the position of these bands indicates a relatively strong double bond character of the P$=$N units in **1–3**. The NH$_2$ scissoring and NH bending vibrations of the amino groups in **2** and **3** appear at 1700 and 1640 cm$^{-1}$, respectively. Broad bands around 3000–3500 cm$^{-1}$ represent the N–H valence vibrations of the amino group in **2** and **3**. Several bands with medium and weak intensity between 2490 and 3300 cm$^{-1}$ in the IR-spectrum of **3** incorporate the N–H valence vibrations of **3** and N–H and C–H vibrations of Et$_3$NHBr and o-C$_6$H$_4$Cl$_2$.

The $^{31}$P NMR spectra of **1**, **2** and **3** exhibit one singlet each. The resonance of **1** (in 1,2-dichlorobenzene) was observed at 7.1 ppm, whereas the signals of **2** and **3** arise at 18.8 and 21.1 ppm, respectively (in 1,2-dichloroethane). These chemical shifts are in agreement with the data reported for similar compounds.[13] The $^{13}$C NMR spectrum of **1** represents a doublet at 168.7 ($^2J_{P-C}$ = 13.78 Hz), which was assigned to the triazine ring. The $^{13}$C NMR spectra of **2** and **3** exhibit the signals of phenyl rings, whereas the triazine-ring signals were not detected.

**Crystal structures.** The crystal structure data and refinement details for **1**, **2** and **3** are summarized in Table S1 (see ESI†).
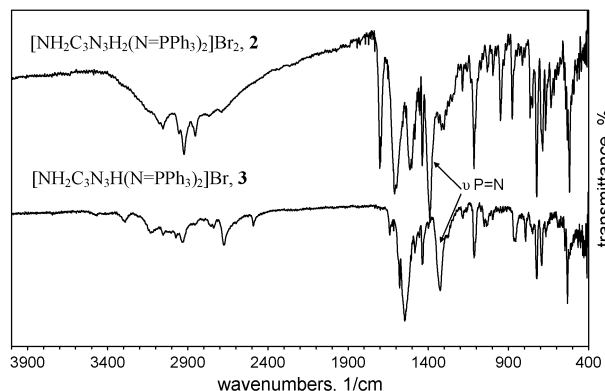
**Fig. 1** IR spectrum of compounds **2** and **3** in the range 400–4000 cm$^{-1}$.

2,4,6-Tris(trichlorophosphinimino)-s-triazine **1** forms colourless single crystals suitable for X-ray analysis upon cooling the reaction solution down to 5 °C. Compound **1** crystallized without solvent molecules in the triclinic space group $P\bar{1}$. The asymmetric unit of **1** comprises two crystallographically independent molecules of **1** (Fig. 2). Both molecules show similar structural parameters, but different spatial orientation. The least-squares planes of the triazine-cores (C1–C3 and C4–C6) are inclined towards each other at an angle of 18.70(4)°.

The molecules of **1** are arranged in layers with an ABAB order parallel to the (011) plane (Fig. 3).

Layer arrangements have already been observed in the crystal structures of related s-triazine derivatives, e.g. cyanuric acid $C_3N_3(OH)_3$,[23] cyanuric chloride $C_3N_3Cl_3$[24] or tris(trimethylsilyl)cyanurate.[25] While the layers in cyanuric acid are held together by hydrogen bonds, the cyanuric chloride structure is characterized by short (3.0 to 3.3 Å)
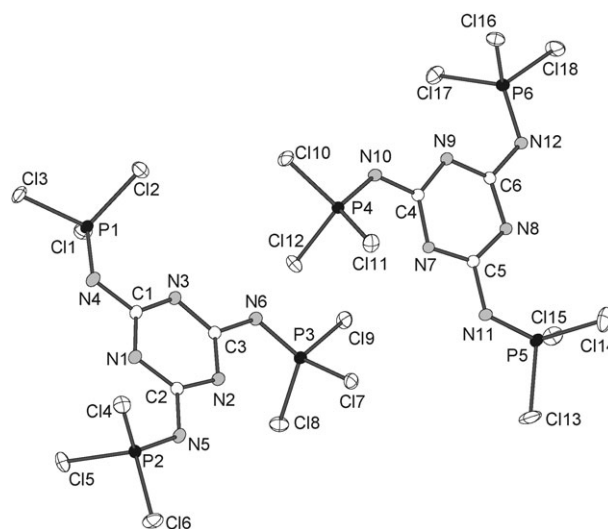
**Fig. 2** Crystal structure and atom numbering scheme of 2,4,6-tris-(trichlorophosphinimino)-s-triazine **1** (thermal ellipsoids at 50% probability).
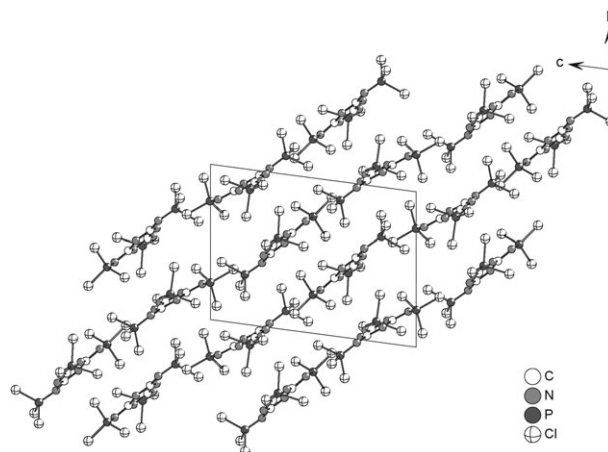
**Fig. 3** The layer structure of 2,4,6-tris(trichlorophosphinimino)-s-triazine **1**, viewed along the a axis.

| **Table 1** Intermolecular Cl···N distances in **1** ($d < 3.3$ Å) | | | |
|---|---|---|---|
| Cl···N distances (Å) | | P–Cl···N angles (°) | |
| Cl3···N12 | 2.943(5) | P1–Cl3···N12 | 175.85(4) |
| Cl6···N6 | 3.196(1) | P2–Cl6···N6 | 157.21(3) |
| Cl10···N5 | 2.986(5) | P4–Cl10···N5 | 168.85(3) |
| Cl18···N11 | 3.215(1) | P6–Cl18···N11 | 157.52(3) |

**Table 2** Selected bond lengths and angles for one of the two independent molecules of **1**

| Bond lengths (Å) | | Bond angles (°) | | | |
|---|---|---|---|---|---|
| P1–N4 | 1.546(1) | C2–N1–C1 | 114.43(12) | N5–P2–Cl4 | 118.22(5) |
| P2–N5 | 1.543(1) | C2–N2–C3 | 113.80(12) | Cl6–P2–Cl4 | 104.84(2) |
| P3–N6 | 1.548(1) | C3–N3–C1 | 114.00(12) | Cl5–P2–Cl4 | 102.76(2) |
| N1–C2 | 1.337(2) | N1–C1–N3 | 125.59(14) | Cl5–P2–Cl4 | 102.76(2) |
| N1–C1 | 1.344(2) | N1–C2–N2 | 125.92(13) | N6–P3–Cl9 | 105.97(5) |
| N2–C2 | 1.342(2) | N3–C3–N2 | 126.26(13) | N6–P3–Cl8 | 117.29(5) |
| N2–C3 | 1.347(2) | N1–C1–N4 | 115.63(13) | Cl9–P3–Cl8 | 104.79(2) |
| N3–C3 | 1.337(2) | N3–C1–N4 | 118.78(13) | N6–P3–Cl7 | 118.96(5) |
| N3–C1 | 1.345(2) | N1–C2–N5 | 118.42(13) | Cl9–P3–Cl7 | 104.19(2) |
| N4–C1 | 1.372(2) | N2–C2–N5 | 115.66(13) | Cl8–P3–Cl7 | 104.08(2) |
| N5–C2 | 1.385(2) | N3–C3–N6 | 115.47(12) | | |
| N6–C3 | 1.382(2) | N2–C3–N6 | 118.26(13) | | |
| Cl1–P1 | 2.0020(6) | N4–P1–Cl3 | 107.95(5) | | |
| Cl2–P1 | 1.9978(5) | N4–P1–Cl2 | 117.52(6) | | |
| Cl3–P1 | 1.9643(6) | Cl3–P1–Cl2 | 104.29(2) | | |
| Cl4–P2 | 1.9920(5) | N4–P1–Cl1 | 117.29(6) | | |
| Cl5–P2 | 1.9916(5) | Cl3–P1–Cl1 | 104.67(3) | | |
| Cl6–P2 | 1.9673(5) | Cl2–P1–Cl1 | 103.70(2) | | |
| Cl7–P3 | 1.9862(5) | N5–P2–Cl6 | 108.31(5) | | |
| Cl8–P3 | 1.9811(5) | N5–P2–Cl5 | 117.37(5) | | |
| Cl9–P3 | 1.9801(5) | Cl6–P2–Cl5 | 103.78(2) | | |

Cl···N interactions.[26] Such interactions were observed in case of triazine systems[24,27] as well as in heptazine chloride,[28,29] and are present in the crystal structure of **1** as well. In the latter case four Cl···N contacts with relatively short (shorter or equal to the sum of the chlorine and nitrogen van der Waals radii, 3.30 Å[30]) interatomic distances are observed (Table 1).

These interactions are found within one layer, *i.e.* the respective P, C and Cl atoms are roughly trigonal planar arranged around the N atoms with the PNC, PNCl and CNCl angles ranging between 110° and 128°.

The triazine motifs of **1** have a slightly distorted hexagonal structure. All three CNC angles in both molecules are very close to 114°, whereas the NCN angles are significantly larger (*ca.* 126°) (Table 2). These angles, together with the bond lengths within the triazine ring of **1**, are similar to those in melamine[31] and in alkali metal melaminates.[32]

The three P=N-groups of **1** are almost in plane with the triazine ring (the deviation from the ring plane does not exceed 0.037(1) Å for N and 0.187(1) Å for P atoms) imparting $C_3$ symmetry to the molecule. A comparison between the C–N(=P) bonds indicates that C1–N4 is slightly shorter than the other two (1.372(2) *vs.* 1.382(2) Å). The fact that the N5 and N6 atoms, contrary to N4, do participate in Cl···N interactions leads to the assumption that the elongation of the C2–N5 and C3–N6 bonds is a consequence of the donor–acceptor interaction between the N5 and N6 and chlorine atoms. A similar effect was found for the other molecule as well. At the same time, the bond parameters of the C1–N4 and C4–N10 are similar to the C–N(=P) bonds in C₃N₃(N=PPh₃)₃,[13b] where nitrogen atoms are not involved in any donor–acceptor contacts.

The P–N bond distances in compounds **1–3**, **5** and **6** (Tables 2 and 4) are typical for a P=N double bond (1.55 Å).[33] But, with respect to a specific nature of the bonding in iminophosphoranes[9,34] a very polar single bond $P^+$–$N^-$ is preferred. Indeed, an analysis of the topological properties of the electron density in **1**, **2**, **5** and **6** shows a predominantly ionic $P^+$–$N^-$ bond character (see quantum chemical analysis below). Therefore we retain the formal "double-bond" P=N throughout the schemes only for simplicity.

The P–N bond lengths in **1** of 1.540(1)–1.554(1) Å are somewhat shorter than those found in C₃N₃(N=PPh₃)₃ (1.588(3) Å),[13b] in the corresponding monomer NCN=PPh₃ (1.595(4) Å),[35] in **2** (~1.615 Å) and in **3** (~1.606 Å). This P–N bond shortening in **1** is enhanced by the electron-withdrawing effect of the Cl-substituents, which increases the $\delta+$ charge on the phosphorus atoms, and in turn the electron donation from the nitrogen to the phosphorus atoms.

2-Amino-4,6-bis(triphenylphosphinimino)triazine dihydrobromide **2** crystallizes in the monoclinic space group $P2_1/n$ with one *o*-dichlorobenzene molecule per molecular unit. The

related compound **3** crystallizes in the triclinic space group $P\bar{1}$ as a triethylamine hydrobromide double salt which comprises 1.5 *o*-dichlorobenzene molecules per molecular unit. The molecular structures of **2**·*o*-C₆H₄Cl₂ and **3**·Et₃NHBr·1.5 *o*-C₆H₄Cl₂ are shown in Fig. 4.

Compounds **2** and **3** consist of the cations [H₂NH₂C₃N₃(N=PPh₃)₂]²⁺ and [HNH₂C₃N₃(N=PPh₃)₂]⁺, respectively, and bromide anions. Interestingly, during the conversion of **2** to **3**, the proton remaining at the s-triazine ring changes its position and protonates the nitrogen atom N1 (Fig. 4).

The deviation of the bromide anion positions from the triazine-ring plane in **2** and **3** is less than 0.7 Å. Bromide anions in **2** and **3** act as hydrogen bond acceptors, forming several N–H···Br contacts with the cation (Fig. 4, Table 3). The Br2 anion in compound **3** suffers disorder with a site occupancy factor (s.o.f.) of 0.97 and 0.03. Site Br2a (s.o.f. 0.03) simulates unusually short contacts to some of the triethylammonium C-atoms. We conclude that the triethylammonium ion is also disordered, but it was not possible to detect the alternative sites with a s.o.f. 0.03 on the residual electron density map.

Additionally, the bromide ions of **2** and **3** form several C–H···Br contacts with neighbouring phenyl rings. The average H···Br distances are about 3.2 Å and the C–H···Br bond angles vary between 110° and 175°.

The triazine motifs of the cationic units [H₂NH₂C₃N₃-(N=PPh₃)₂]²⁺ and [HNH₂C₃N₃(N=PPh₃)₂]⁺ are planar, since the sum of the bond angles around the N and C atoms are close to 360°; the phosphorus atoms exhibit slightly distorted tetrahedral geometry (Table 4). The hexagonal structure of the triazine rings suffers some distortion under the influence of protonation. Consistent with the VSEPR concept, the CNC angles at the protonated nitrogen atoms are somewhat greater than the others. Similar effects were observed in various melamine salts.[36] The C1–N2 and C3–N3
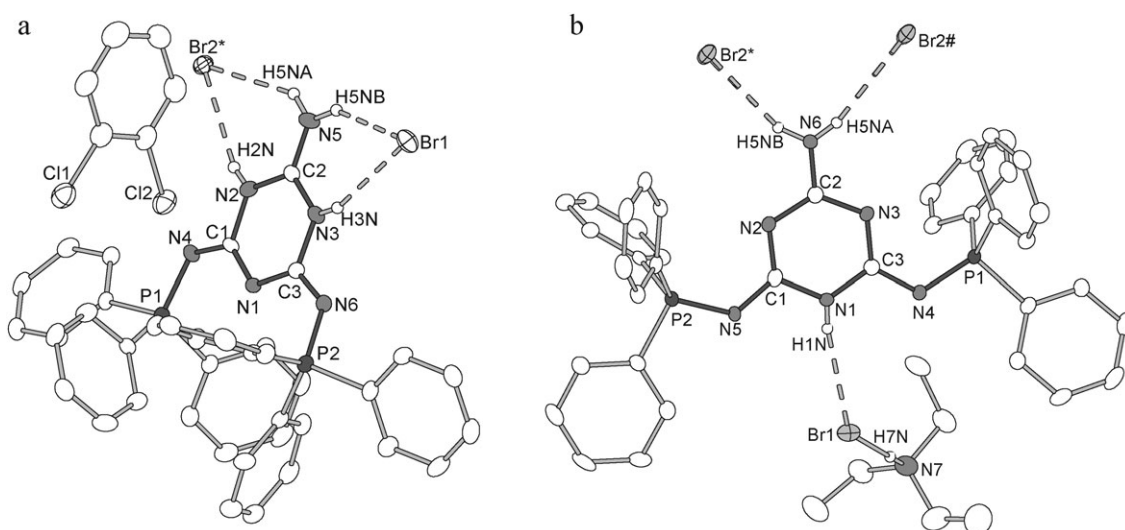
**Fig. 4** Molecular structure and the atom numbering scheme of (a) 2-amino-4,6-bis(triphenylphosphinimino)triazine dihydrobromide $2 \cdot o\text{-}C_6H_4Cl_2$ (position Br2* is generated from Br2 by symmetry operation $(1 - x, 2 - y, 1 - z)$) and (b) 2-amino-4,6-bis(triphenylphosphinimino)triazine hydrobromide $3 \cdot Et_3NHBr \cdot 1.5 \, o\text{-}C_6H_4Cl_2$ ($o\text{-}C_6H_4Cl_2$ molecules are omitted for clarity; positions Br* and Br2# are generated from Br2 by symmetry operation $(1 - x, 1 - y, -z)$ and $(x - 1, y - 1, z)$, respectively); thermal ellipsoids at 50% probability.

**Table 3** Geometric parameters of the selected hydrogen bonds in $2 \cdot o\text{-}C_6H_4Cl_2$ and $3 \cdot Et_3NHBr \cdot 1.5 \, o\text{-}C_6H_4Cl_2$. The position of Br2* is generated from Br2 by symmetry operation $(1 - x, 2 - y, 1 - z)$ for compound $2 \cdot o\text{-}C_6H_4Cl_2$ and positions Br* and Br2# are generated from Br2 by symmetry operations $(1 - x, 1 - y, -z)$ and $(x - 1, y - 1, z)$ for compound $3 \cdot Et_3NHBr \cdot 1.5 \, o\text{-}C_6H_4Cl_2$

| D–H···A (°) | D–H (Å) | H···A (Å) | D···A (Å) | ∠ D–H···A (°) |
|---|---|---|---|---|
| 2-Amino-4,6-bis(triphenylphosphinimino)triazine dihydrobromide **2** | | | | |
| N2–H2N···Br2* | 0.72(4) | 2.56(4) | 3.244(3) | 155(4) |
| N3–H3N···Br1 | 0.74(3) | 2.54(3) | 3.214(3) | 153(3) |
| N5–H5NA···Br2* | 0.83(4) | 2.64(3) | 3.335(4) | 143(2) |
| N5–H5NB···Br1 | 0.90(5) | 2.51(4) | 3.305(3) | 148(4) |
| 2-Amino-4,6-bis(triphenylphosphinimino)triazine hydrobromide **3** | | | | |
| N1–HN1···Br1 | 0.72(3) | 2.76(3) | 3.460(2) | 163(3) |
| N6–H5NB···Br2* | 0.86(2) | 2.54(2) | 3.349(2) | 158(3) |
| N6–H5NA···Br2# | 0.80(3) | 2.81(3) | 3.577(3) | 163(3) |
| N7–HN1···Br1 | 1.02(3) | 2.29(3) | 3.308(3) | 176(2) |

bonds of **2** (1.386(4) Å) are significantly longer than those in **3** (1.332(3) Å) and in **1** (1.342(2) Å), with almost a single-bond distance (1.39 Å).[37] In contrast, in the case of **3** the C1–N1 and C3–N1 bond lengths are somewhat elongated in comparison with those of **1** and **2**.

The C–N(=P) and C–NH$_2$ bond distances in both compounds have similar values, varying around 1.309(4) Å in **2** and 1.331(3) Å in **3**. These bonds are only slightly longer than the isolated C=N double bonds (1.27 Å).[37]

The P=N bond lengths in both salts vary between 1.604(3) and 1.623(3) Å, being in agreement with a partial double bond character of the phosphinimino-groups. Similar bond lengths of the $C_{triazine}$–P=N motif were observed in $C_3N_3(N=PPh_3)_3$.[13a] The iminophosphorane-substituents in **2** and **3** are aligned in such a way that the Ph$_3$P groups do not hinder the protons accommodation by the triazine ring. Dihedral angles P–N···N–P in **2** and **3** comprise 17.6° and 20.2°, respectively.

As mentioned above, the treatment of **2** or **3** with Ph$_3$PBr$_2$ in 1,2-dichloroethane did not result in the formation of threefold phosphinimino-substituted triazines but in partial halide exchange between the solvent and Ph$_3$PBr$_2$. The asymmetric unit of the chlorotriphenylphosphonium chloride/bromide **4** consists of 1/3 of the unit $[(PPh_3PCl)^+X^- \cdot C_2H_4Cl_2]$, *i.e.*, the rest of the Ph$_3$PCl-cation is generated by a threefold rotation axis, which includes the P–Cl bond. The 1,2-dichloroethane molecule is threefold disordered by symmetry (as well as statistically in a 1 : 1 ratio). The anion occupies two crystallographically different sites: the first position comprises 92% bromide and 8% chloride occupancy, and second site reveals occupancies of 65% for bromide and 35% for chloride. Thus, the molecular composition of **4** has to be written as $[(PPh_3PCl)^+(Br_{0.79}Cl_{0.21})^- \cdot C_2H_4Cl_2]$. Crystallographic data of **4** is represented in the supplementary information†.

**s-Heptazine-based iminophosphoranes**

In contrast to melamine, which has been investigated in detail, there exists far less knowledge about the reactivity of melem. This also holds true for reactions of these amines with compounds containing P-halogen bonds. The high thermal stability of melem (up to 450 °C[38]) and chemical inactivity of its amino-groups[39] hinders the syntheses of further N-substituted derivatives thereof and renders them very interesting targets at

**Table 4** Selected bond lengths (Å) and angles (°) for $2 \cdot o\text{-}C_6H_4Cl_2$ and $3 \cdot Et_3NHBr \cdot 1.5\ o\text{-}C_6H_4Cl_2$

| 2 | | 3 | |
|---|---|---|---|
| P1–N4 | 1.622(3) | P1–N4 | 1.607(2) |
| P2–N6 | 1.609(3) | P2–N5 | 1.604(2) |
| N1–C1 | 1.345(4) | N1–C1 | 1.377(3) |
| N1–C3 | 1.345(4) | N1–C3 | 1.359(3) |
| N2–C2 | 1.336(4) | N2–C2 | 1.351(3) |
| N2–C1 | 1.386(4) | N2–C1 | 1.336(3) |
| N3–C3 | 1.388(4) | N3–C3 | 1.332(3) |
| N4–C1 | 1.309(4) | N4–C3 | 1.339(3) |
| N5–C2 | 1.311(4) | N6–C2 | 1.331(3) |
| N6–C3 | 1.307(4) | N5–C1 | 1.328(3) |
| C1–N1–C3 | 118.7(3) | C1–N1–C3 | 121.3(2) |
| C2–N2–C1 | 121.9(3) | C2–N2–C1 | 115.8(2) |
| C2–N3–C3 | 122.6(3) | C2–N3–C3 | 116.1(2) |
| N1–C1–N2 | 120.3(3) | N1–C1–N2 | 119.9(2) |
| N2–C2–N3 | 116.6(3) | N2–C2–N3 | 126.7(2) |
| N1–C3–N3 | 119.5(3) | N1–C3–N3 | 120.2(2) |
| N4–C1–N1 | 126.1(3) | N5–C1–N1 | 115.1(2) |
| N4–C1–N2 | 113.6(3) | N5–C1–N2 | 125.0(2) |
| N5–C2–N2 | 122.1(3) | N6–C2–N2 | 116.8(2) |
| N5–C2–N3 | 121.3(3) | N6–C2–N3 | 116.4(2) |
| N6–C3–N1 | 127.3(3) | N4–C3–N1 | 116.5(2) |
| N6–C3–N3 | 113.3(3) | N4–C3–N3 | 123.3(2) |
| C1–N4–P1 | 123.4(2) | C1–N5–P2 | 124.1(2) |
| C3–N6–P2 | 129.8(2) | C3–N4–P1 | 119.5(2) |
| C2–N2–H2N | 118(3) | C1–N1–H1N | 116(2) |
| C1–N2–H2N | 120(3) | C3–N1–H1N | 123(2) |
| H5NA–N5–H5NB | 115(3) | H5NA–N6–H5NB | 120(3) |
| C2–N5–H5NA | 124(3) | | |
| C2–N5–H5NB | 121(2) | | |
| C2–N3–H3N | 121(3) | | |
| C3–N3–H3N | 116(3) | | |

the same time. There is only one example of the Kirsanov reaction, for the synthesis of the 2,5,8-tris(trichlorophosphinimino)-s-heptazine **5** from melem and PCl$_5$, which was referred to in a patent application by our group.[8f,14a] In further studies we optimized the reaction conditions and essentially increased the yield of the reaction. Here we report this approach more elaborately and provide detailed characterization of the obtained product. The reactivity of the P–Cl bonds of **5** was tested by its reaction with phenol. Relatively fast and
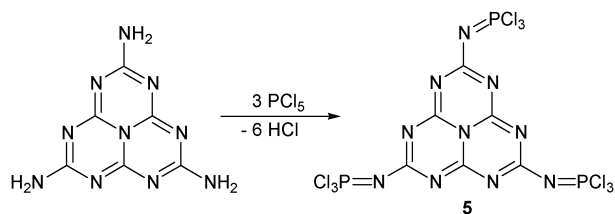


**Scheme 7** Synthesis of 2,5,8-tris(trichlorophosphinimino)-s-heptazine **5**.
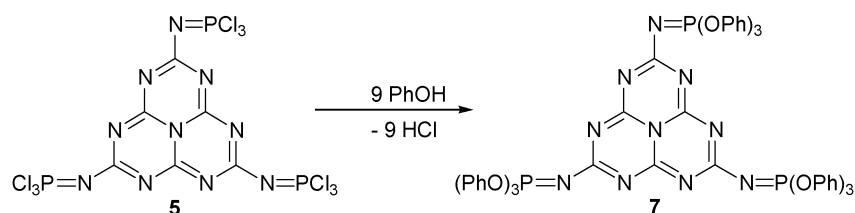
uncomplicated synthesis resulted in tris(2,5,8-triphenoxy-phosphinimino)-s-heptazine **7**. This compound was successfully tested as a halogen-free fire retardant (see below).

**Synthesis and spectroscopic characterisation.** Compound **5** was synthesized in a similar manner to **1** (Scheme 7).

2,5,8-Tris(trichlorophosphinimino)-s-heptazine **5** is a white to slightly yellow solid, soluble in THF and polar halogenated solvents. Its behaviour towards water and alcohols is similar to **1**, i.e., nucleophilic attack at phosphorus takes place.

Compound **5** reacts exothermically with alcohols and phenols to give alkoxy or aryloxyiminophosphorane derivatives with the formation of HCl gas. The relatively low melting point together with good solubility and high reactivity makes **5** a good starting substrate for further derivatisation. Thus, by reaction with phenol, tris(2,5,8-triphenoxyphosphinimino)-s-heptazine **7** was obtained (Scheme 8).

Compound **7** was isolated as a yellow solid, soluble in polar organic solvents. It was characterised by means of NMR and IR-spectroscopy and thermogravimetric analysis. By recrystallization of the reaction product **5** from 1,2-dichloroethane, colourless crystals of **6** were obtained (Fig. 5). According to the single-crystal X-ray diffraction analysis of **6**, it is an ionic species, consisting of the cation $[C_6N_7H(N{=}PCl_3)_3]^+$ and a chloride counterion. **6** is a by-product, which was formed during the synthesis of 2,5,8-tris(trichlorophosphinimino)-s-heptazine **5** by protonation of one N-atom. The HCl molecule can be removed under vacuum at 100 °C, giving the main product **5**.

The fact that protonation occurs at the heptazine ring, leaving the P=N-groups unaffected, is evidence of the higher basicity of the ring-N atoms. An analogous observation was reported recently for melem itself, as it is protonated by $HClO_4$ and $H_2SO_4$ at the ring-N atoms.[40]

IR spectra of **5**, **6** and **7** are depicted in Fig. 6. The stretching vibrations of the heptazine ring of both compounds **5** and **6** appear as three strong bands at 1625, 1430 and 1270 cm$^{-1}$.

Similar positions for the heptazine stretching vibrations were observed for **7**: 1630, 1415 and 1310 cm$^{-1}$. Stretching vibrations of the P=N-groups in **5** and **6** occur at 1370 and 1395 cm$^{-1}$, i.e., similar to **1**. In the IR spectrum of **7** this band appears at 1390 cm$^{-1}$. The P–Cl stretching, which is represented by a medium vibration at 579 cm$^{-1}$ in **5** and **6**, completely disappears in the case of **7**, which is evidence of the complete substitution of the Cl-atoms with phenoxy groups. The NH-group of **6** is represented by a bending vibration at 1674 cm$^{-1}$ and a broad stretching band at 2800–3100 cm$^{-1}$.

$^{31}$P NMR spectra of **5** and **6** reveal single peaks at 19.2 and 22.3 ppm, respectively. Both signals are shifted downfield with respect to **1**. This can be explained by a more pronounced
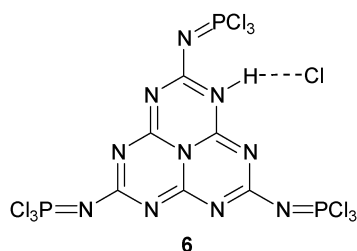


**Scheme 8** Synthesis of tris(2,5,8-triphenoxyphosphinimino)-s-heptazine **7**.

**Fig. 5** 2,5,8-Tris(trichlorophosphinimino)-s-heptazine hydrochloride **6**.
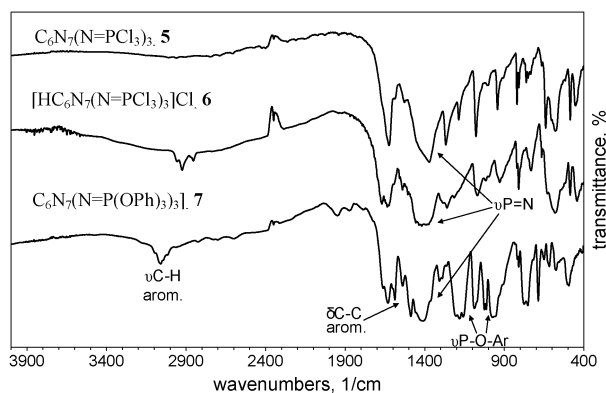


**Fig. 6** IR spectra (KBr pellet) of **5**, **6** and **7** in the range 400–4000 cm$^{-1}$.

electron-withdrawing behaviour of heptazine units relative to triazine units, which leads to a deshielding of the phosphorus nuclei.

The $^{31}$P NMR signal of **7** is strongly shifted upfield relative to the signal of **5**, and appears at −5.9 ppm. Clearly, upon replacement of the Cl substituents on phosphorus by the phenoxy groups the shielding of the P-atom significantly increases. Similar chemical shift values were reported for R–N=P(O-aryl)$_3$ compounds.[41]

The $^{13}$C NMR spectrum of **5** shows two sharp signals with low intensity at 167.5 and 156.5 ppm, which were assigned to the heptazine ring. The same positions of these signals were observed in the $^{13}$C-spectrum of **6**. This fact can be explained by rapid proton exchange between the protonated (**6**) and non-protonated (**5**) species in solution, resulting in domination by the form **5**. The same observation concerns the solution $^{1}$H NMR spectrum of **6**, where no N–H signal was detected. In the $^{13}$C NMR spectrum of **7** only signals of phenoxy groups with characteristic P–C coupling were observed, whereas the heptazine signals were not detectable.

**Crystal structures.** The crystallographic data and refinement details for compounds **5** and **6** are summarized in Table S1 (see ESI†). 2,5,8-Tris(trichlorophosphinimino)-s-heptazine **5** (Fig. 7) crystallizes in the trigonal space group R3c with one o-dichlorobenzene molecule per heptazine molecular unit and six molecular units in the unit cell. Selected bond lengths and angles for **5** are given in Table 5. The asymmetric unit of **5** consists of 1/3 of a C$_6$N$_{10}$P$_3$Cl$_9$ molecule, whereas the rest of the molecule is generated by a threefold axis, which intersects the plane of the molecule in atom N3. The o-dichlorobenzene
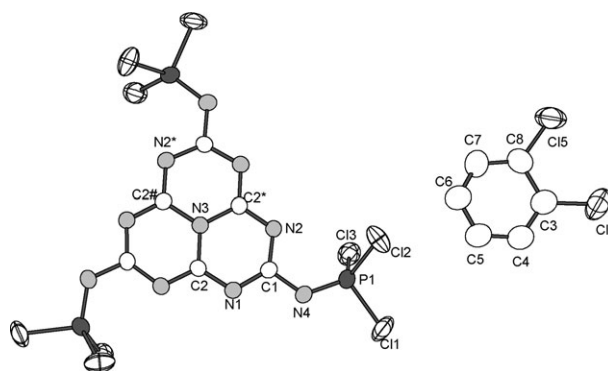


**Fig. 7** Molecular structure of **5**·C$_6$H$_4$Cl$_2$ (thermal ellipsoids at 50% probability; positions * and # are generated by symmetry operations (−y, x − y, z) and (−x + y, −x, z), respectively).

**Table 5** Selected bond lengths and angles for **5** in the crystal structure of **5**·o-C$_6$H$_4$Cl$_2$

| Bond lengths (Å) | | Bond angles (°) | |
|---|---|---|---|
| P1–N4 | 1.543(3) | C2–N1–C1 | 117.1(2) |
| N1–C1 | 1.335(4) | C2*–N2–C1 | 117.2(2) |
| N1–C2 | 1.326(4) | C2–N3–C2* | 120.00(1) |
| N2–C1 | 1.346(4) | N1–C1–N2 | 127.0(3) |
| N2–C2* | 1.328(4) | N1–C1–N4 | 114.6(2) |
| N3–C2# | 1.405(3) | N2–C1–N4 | 118.3(3) |
| N4–C1 | 1.368(4) | N1–C2–N2# | 121.5(3) |
| Cl1–P1 | 1.969(1) | N1–C2–N3 | 119.5(2) |
| Cl2–P1 | 1.967(1) | N2–C2*–N3 | 119.0(2) |
| Cl3–P1 | 1.993(1) | N4–P1–Cl2 | 118.9(1) |
| | | N4–P1–Cl1 | 106.2(1) |
| | | N4–P1–Cl3 | 117.1(1) |

molecule (1/3 of the asymmetric unit) is situated on a threefold axis as well, hence the threefold disordered symmetry. Thus, restraints of equal C–Cl bond lengths and identical C–C bonds were applied in the refinement. Therefore, the bonding parameters of the o-dichlorobenzene molecule are reasonable, but not appropriate for discussion.

The molecules of **5** are arranged in layers parallel to the [001] plane, in an ABCA′B′C′A order (Fig. 8). The heptazine units of molecules of the A and A′, B and B′, and C and C′ layers, are situated directly one above the other (Fig. 9). The heptazine moieties of the layers are sandwiched by solvent molecules. The distances between the heptazine cores are about 7 Å, whereas the heptazine–benzene planes are
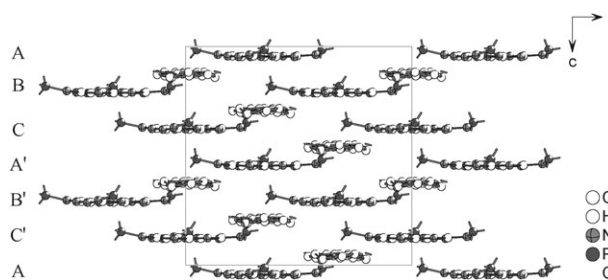


**Fig. 8** Layer structure of the compound **5** in the crystal structure of **5**·o-C$_6$H$_4$Cl$_2$ viewed along the b axis. The chlorine atoms are omitted for clarity.
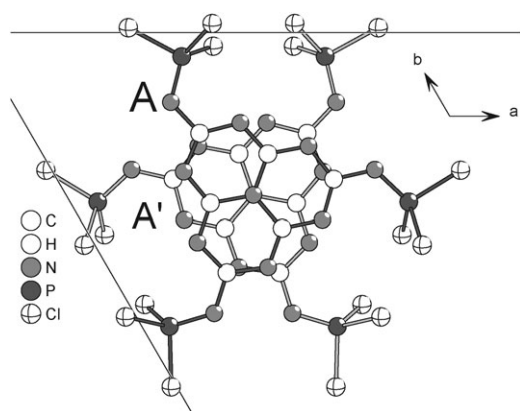
**Fig. 9** The molecules of the A and A′ layers of the compound **5** in the crystal structure of **5**·o-C₆H₄Cl₂. The solvent molecules are omitted for clarity.

separated by 3.482(3)–3.834(3) Å, with an angle between the planes of about 7.5°, providing suitable spatial characteristics for weak π–π-interaction.

The s-heptazine skeleton $C_6N_7$ is planar, as indicated from the sum of the angles, 360 (±0.2)°, around the C1, C2 and N3 atoms. This finding is in accordance with known examples of s-heptazine derivatives.[29,42] The bonding character and geometry of the s-heptazine rings are in agreement with the relatively few known examples of s-heptazine derivatives (see Table 1 in ref. 42a). Geometrical characteristics of the C–N=P fragment in **5** are very similar to those in **1**. The P–N distance of 1.543(3) Å illustrates double bond character between the phosphorus and the nitrogen atoms as discussed above for compound **1**.

In the case of **5**, as well as in the case of **1**, the crystal structure is influenced by several Cl···N interactions. There are four such contacts per asymmetric unit, *i.e.* twelve for the whole molecule of **5** (Table 6).

In contrast to **1**, there are no N···Cl interactions within the layers. All observed N···Cl contacts appear between the molecules of different layers, and are longer than in the case of **1**.

The ionic compound 2,5,8-tris(trichlorophosphinimino)-s-heptazine hydrochloride **6** crystallizes in the monoclinic space group $P2_1/n$, including one 1,2-dichloroethane molecule in the asymmetric unit (Fig. 10). Geometric parameters of **6** are summarized in Table 8. Compound **6** consists of the cation [C₆N₇H(N=PCl₃)₃]⁺ and a Cl⁻ anion, which interact with one another *via* the hydrogen bridge N4–H1···Cl12.

A computational study, performed for the hydrogen bridged tri-s-triazine molecule and a Cl⁻ anion (C$_{hept.}$–H···Cl),

**Table 6** Intermolecular N···Cl distances and angles found in the crystals of **5**·o-C₆H₄Cl₂ with d < 3.5 Å

| Bond lengths (Å) | | Bond angles (°) | |
|---|---|---|---|
| N1···Cl1 | 3.324(2) | N1···Cl1–P1 | 132.09(7) |
| N1···Cl2 | 3.175(3) | N1···Cl2–P1 | 156.67(7) |
| N4···Cl2 | 3.170(4) | N4···Cl2–P1 | 155.26(8) |
| N4···Cl3 | 3.452(4) | N4···Cl2–P1 | 143.90(8) |

**Table 7** Geometric parameters of the hydrogen bonds in **6**·C₂H₄Cl₂

| D–H···A (°) | D–H (Å) | H···A (Å) | D···A (Å) | D–H···A (°) |
|---|---|---|---|---|
| N4–H4N···Cl12 | 0.94(3) | 2.06(3) | 2.994(2) | 177(2) |
| C8–H8A···Cl12 | 0.99 | 2.70 | 3.471(2) | 135 |

**Table 8** Selected bond lengths and angles for **6**·C₂H₄Cl₂

| Bond lengths (Å) | | Bond angles (°) | |
|---|---|---|---|
| P1–N8 | 1.567(2) | N1–C1–N8 | 116.4(2) |
| P2–N9 | 1.557(2) | N1–C1–N6 | 126.2(2) |
| P3–N10 | 1.560(2) | N8–C1–N6 | 117.4(2) |
| N1–C2 | 1.323(2) | N1–C2–N2 | 120.5(2) |
| N1–C1 | 1.346(2) | N1–C2–N7 | 120.3(2) |
| N2–C2 | 1.333(2) | N2–C2–N7 | 119.2(2) |
| N2–C3 | 1.339(2) | N2–C3–N9 | 119.5(2) |
| N3–C4 | 1.307(2) | N2–C3–N3 | 126.3(2) |
| N3–C3 | 1.367(2) | N9–C3–N3 | 114.2(2) |
| N4–C4 | 1.354(2) | N3–C4–N4 | 120.8(2) |
| N4–C4 | 1.363(2) | N3–C4–N7 | 122.9(2) |
| N5–C5 | 1.326(2) | N4–C4–N7 | 116.2(2) |
| N5–C6 | 1.342(2) | N5–C5–N10 | 121.9(2) |
| N6–C6 | 1.309(2) | N5–C5–N4 | 123.5(2) |
| N6–C1 | 1.360(2) | N10–C5–N4 | 114.6(2) |
| N7–C4 | 1.380(2) | N6–C6–N5 | 120.3(2) |
| N7–C6 | 1.396(2) | N6–C6–N7 | 119.3(2) |
| N7–C2 | 1.400(2) | N5–C6–N7 | 120.4(2) |
| N8–C1 | 1.357(2) | Cl1–P1–Cl3 | 105.88(4) |
| N9–C3 | 1.359(2) | Cl2–P1–Cl3 | 106.26(4) |
| N10–C5 | 1.345(2) | N9–P2–Cl6 | 106.30(7) |
| Cl1–P1 | 1.9605(7) | N9–P2–Cl4 | 117.90(7) |
| Cl2–P1 | 1.9835(9) | Cl6–P2–Cl4 | 105.90(3) |
| Cl3–P1 | 1.9852(8) | N9–P2–Cl5 | 117.63(8) |
| Cl4–P2 | 1.9790(7) | Cl6–P2–Cl5 | 104.09(3) |
| Cl5–P2 | 1.9863(7) | Cl4–P2–Cl5 | 103.68(3) |
| Cl6–P2 | 1.9706(7) | N10–P3–Cl7 | 105.88(6) |
| Cl7–P3 | 1.9550(7) | N10–P3–Cl9 | 115.79(7) |
| Cl8–P3 | 1.9785(7) | Cl7–P3–Cl9 | 106.25(3) |
| Cl9–P3 | 1.9872(8) | | |

suggested H···Cl distances of 2.266 (2.234) Å,[43] whereas the value observed in **6** does not exceed 2.06(3) Å (Table 7). This fact together with the N–H···Cl bond angle of 176.5° is evident of relatively strong hydrogen bonding in **6**.

The arrangement of the ions of salt **6** may be considered as a chain structure, where the chains are aligned in the [101] plane (Fig. 10). The intermolecular interaction within the chains occurs *via* short N8···Cl7 contacts between neighbouring molecules. Inter-chain contacts occur between the heptazine π system and a Cl12 anion. The parameters of the N···Cl contacts, including interactions with the solvent, are listed in Table 9.

Distances between the anion and the central N-atom of the heptazine ring N7···Cl12 are only slightly longer than the predicted value (3.067 Å).[43]

The orientation of the phosphinimino groups in **6** is different from those observed for **5**. Two of them, N8=P1 and N10=P3, are pointing in the same direction with a dihedral angle of 3.5°. The N9=P2 unit exhibits a dihedral angle of 137° with the P1=N8 moiety and 9.4° with the N10=P3 group. Both, the C–N and the P=N bond distances in **6** are considerably elongated relative to **5**, this may be a consequence of the heptazine ring protonation and partial loss of its aromaticity.
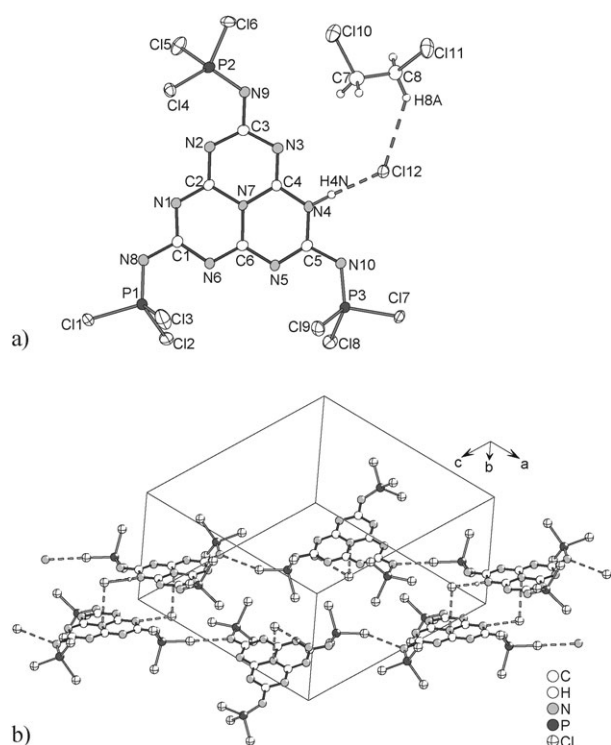
**Fig. 10** (a) Molecular unit and numbering scheme of compound **6** in the crystal structure of **6**·C₂H₄Cl₂ (thermal ellipsoids of 50% probability; the atomic labels of the dichloroethane molecule correspond to the asymmetric unit, but the atomic coordinates were generated by symmetry operation ($-x$, $2 - y$, $1 - z$); the Cl12 atom was generated by symmetry operation ($x - 1$, $1 + y$, $z$); (b) the chain-like structure of **6** (two chains are shown; the solvent molecules are omitted for clarity).

**Table 9** Intermolecular N···Cl distances found in the crystals of **6**·C₂H₄Cl₂ with $d < 3.3$ Å

| Distances (Å) | | Angles (°) | |
|---|---|---|---|
| N8···Cl7 | 3.029(2) | N8···Cl7–P3 | 156.99(5) |
| N4···Cl10 | 3.187(2) | N4···Cl10–C7 | 128.48(9) |
| N10···Cl12 | 3.589(3) | C2–N7···Cl12 | |
| N7···Cl12 | 3.240(3) | C4–N7···Cl12 | |
| | | C6–N7···Cl12 | Average: 88.96(11) |

## Quantum chemical analysis

The electronic structures of triazine[44] and heptazine and some of their derivatives[43,45,46] have been studied earlier with quantum chemical methods. The conjugated system of the heptazine unit has a very strong positive electrostatic potential,[45] which makes the ring suitable as a receptor for anion recognition.[43]

The interesting rearrangement of the proton during the deprotonation of **2** and formation of **3** in solution is evidence of the thermodynamic stability of this tautomer. This fact motivated us to perform calculations of the relative energy of **3** and its possible isomers (Fig. 11). In order to distinguish experimental from optimized geometries, the latter were denoted in the computational analyses as **3a–d**.

As follows from the energy calculations, compound **3a** is the most stable isomer. For instance, the formal product of direct deprotonation of **2**, isomer **3c**, is 65.2 kJ mol⁻¹ higher in energy than **3a**. Two further isomers **3b** and **3d** with modified positions of triphenylphosphinimino substituents show relatively high energy as well. Therefore we can assume, that the stability of **3a** results from the symmetrical conjugated system of double bonds and the favourable position of the Ph₃P=N– substituents. The rearrangement of the remaining proton should be possible, since the deprotonation from **2** to **3** occurs in solution.

The combination of the triazine or heptazine unit with phosphinimine substituents yields intriguing systems, which deserve further consideration. Density functional theory has been used here to study the electronic structure and the topological properties of the electron density distribution of **2**, **3**, **5**, and **6**. These compounds with optimized geometries were denoted as **2a**, **2b**, **3a**, **5a**, and **6a** respectively. The optimized geometries are in good agreement with the experimental data (see ESI†).

The topology of the molecular charge distribution was analyzed with the Quantum Theory of Atoms in Molecules (QTAIM).[47–49] This method delivers unique information about the bonding degree between two atoms from the electron density ($\rho$) and the ellipticity ($\varepsilon$) of the electron density distribution at the bond critical point (BCP).[49] Further information about the covalent or ionic character of the bond can be drawn from the Laplacian of the electron density ($\nabla^2\rho$) at the BCP and suitable graphical representations of this property. In order to see the changes in the bonding situation, the topological properties of **2a** and **3a** are listed together with the properties of the parent compound **2b** in Table 10 and Fig. 13. The values for a C–N single and a C=N double bond have been added from simple model compounds for
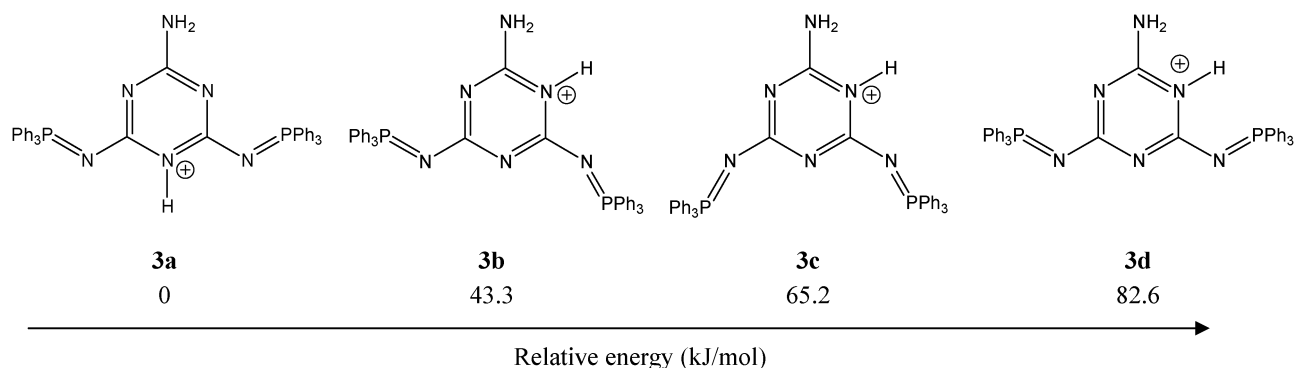


| **3a** | **3b** | **3c** | **3d** |
|---|---|---|---|
| 0 | 43.3 | 65.2 | 82.6 |

Relative energy (kJ/mol)

**Fig. 11** Calculated energy differences (kJ mol⁻¹) between isomers of **3**. Charges are designated as formal charges.

**Table 10** Charge density ($\rho$), Laplacian ($\nabla^2\rho$), and ellipticity ($\varepsilon$) at bond critical points (BCP) in atomic units (same atom numbering as in the X-ray structures)

| BCP | $\rho$ | | | $\nabla^2\rho$ | | | $\varepsilon$ | | |
|---|---|---|---|---|---|---|---|---|---|
| | **2a** | **3a** | **2b** | **2a** | **3a** | **2b** | **2a** | **3a** | **2b** |
| N1–C3 | 0.348 | 0.313 | 0.340 | −1.229 | −1.016 | −1.188 | 0.162 | 0.114 | 0.149 |
| C3–N3 | 0.273 | 0.353 | 0.347 | −0.812 | −1.275 | −1.246 | 0.085 | 0.158 | 0.153 |
| C2–N3 | 0.349 | 0.347 | 0.355 | −1.230 | −1.236 | −1.286 | 0.194 | 0.128 | 0.136 |
| C2–N5 | 0.350 | 0.337 | 0.324 | −1.205 | −1.109 | −1.102 | 0.211 | 0.162 | 0.137 |
| C3–N6 | 0.374 | 0.356 | 0.322 | −1.192 | −1.258 | −1.101 | 0.235 | 0.167 | 0.102 |
| N6–P2 | 0.176 | 0.187 | 0.201 | 0.549 | 0.596 | 0.811 | 0.004 | 0.030 | 0.057 |
| N3–H | 0.340 | — | — | −1.850 | — | — | 0.039 | — | — |
| N1–H | — | 0.343 | — | — | −1.858 | — | — | 0.041 | — |
| | **6a** | **5a** | | **6a** | **5a** | | **6a** | **5a** | |
| N7–C4 | 0.314 | 0.294 | | −1.017 | −0.886 | | 0.118 | 0.074 | |
| C4–N4 | 0.326 | 0.362 | | −1.113 | −1.322 | | 0.174 | 0.173 | |
| N4–C5 | 0.312 | 0.353 | | −1.008 | −1.277 | | 0.116 | 0.142 | |
| C5–N5 | 0.366 | 0.346 | | −1.330 | −1.232 | | 0.190 | 0.139 | |
| N5–C6 | 0.345 | 0.360 | | −1.229 | −1.313 | | 0.144 | 0.178 | |
| C6–N7 | 0.290 | 0.294 | | −0.872 | −0.885 | | 0.074 | 0.074 | |
| N4–H1 | 0.338 | — | | −1.852 | — | | 0.039 | — | |
| C5–N10 | 0.342 | 0.318 | | −1.206 | −1.088 | | 0.139 | 0.097 | |
| N10–P3 | 0.205 | 0.213 | | 0.800 | 0.897 | | 0.069 | 0.099 | |
| P3–Cl7 | 0.149 | 0.142 | | −0.225 | −0.228 | | 0.066 | 0.067 | |
| P3–Cl8 | 0.144 | 0.137 | | −0.239 | −0.226 | | 0.017 | 0.010 | |
| P3–Cl9 | 0.144 | 0.137 | | −0.239 | −0.226 | | 0.017 | 0.010 | |
| | Methylamine | | | Methylamine | | | Methylamine | | |
| C–N | 0.267 | | | −0.753 | | | 0.041 | | |
| N–H | 0.341 | | | −1.732 | | | 0.052 | | |
| | $H_2C{=}NH$ | | | $H_2C{=}NH$ | | | $H_2C{=}NH$ | | |
| C=N | 0.389 | | | −0.706 | | | 0.237 | | |
| N–H | 0.337 | | | −1.720 | | | 0.020 | | |
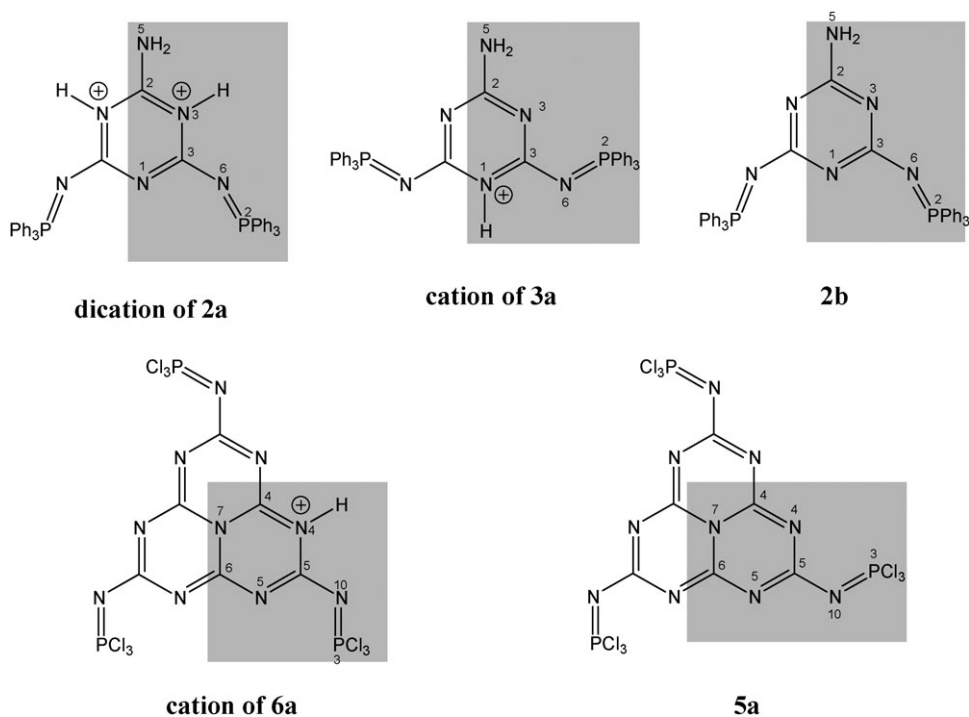


**Fig. 12** Molecules and cations used for topological analyses of electron density. Charges are designated here as formal charges. The grey marked areas are discussed in detail (see text).

comparison. Due to the symmetry of **2a**, **3a** and **2b** only half of the six-membered rings must be considered (grey area in Fig. 12).

There is a rather balanced electron density at the BCPs in the six-membered ring of **2b**, with values between 0.34 and 0.355 e Bohr$^{-3}$ (see Fig. 13 and Table 10) which represent
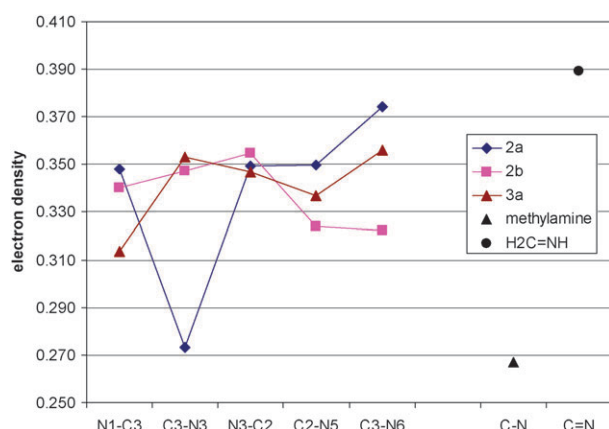
**Fig. 13** Electron density (e Bohr$^{-3}$) at bond critical points in **2a**, **2b**, **3a** methylamine, and H$_2$C=NH (atom numbering according to the X-ray structure of **2**, see Fig. 4).



**Fig. 14** Electron density (e Bohr$^{-3}$) at bond critical points in **5a**, **6a**, methylamine, and H$_2$C=NH (atom numbering according to the X-ray structure of **6**, see Fig. 10).

conjugated double bonds. The exocyclic bonds have substantially lower electron density at 0.324 (C2–N5) and 0.322 e Bohr$^{-3}$ (C3–N6). The protonation of N3 leads to changes in the electron density distribution in **2a**. Most obvious is the drastic lowering of the electron density at the BCP between C3 and N3. The calculated value of 0.273 e Bohr$^{-3}$ is very close to the value of the single bond in methylamine. This lowering of the bonding degree correlates with a longer C3–N3 bond. The bonds N1–C3 and N3–C2 have nearly the same values of electron density as in **2b**, whereas the exocyclic bonds C2–N5 and C3–N6 show higher electron densities. Therefore we can conclude that the protonation of **2b** to **2a** leads to a charge depletion at the bond N3–C3 and a concentration of charge density at the periphery of the cation.

Another situation occurs in the case of the monocation **3a**. Protonation at N1 in **3a** leads to decreasing of the electron density at the BCP between N1 and C3. This electron density lowering is not so pronounced as in the case of **2a**, being between the single-bond and the double-bond values. The other values of the electron density in the six-membered ring are similar to those found for **2b**. The electron density at the BCPs C2–N5 and C3–N6 are between the values of neutral compound **2b** and dication **2a**, as one would expect for the monocation **3a**.

Bond ellipticities at the BCPs support the above discussion. There is a uniform ellipticity of the conjugated bonds in the six-membered ring of **2b**. This situation changes drastically in **2a**. The ellipticity of the bond C3–N3 drops to a value of 0.085, which is very close to the value of the single bond in methylamine. The ellipticity of the N1–C3 in **3a** is 0.114, which is somewhat lower than the other bonds in the triazine-ring of **3a**, but still too high for a single bond. Thus, for the N1–C3 bond in **3a** an intermediate bond order between one and two is assumed.

The electron density distribution in the heptazine system **5a** has two types of bonds: (a) the conjugated double bonds at the outer radius of the heptazine system with electron density values between 0.346 and 0.362 e Bohr$^{-3}$ and (b) the bonds connecting the central nitrogen atom N7 with the carbon atoms, which exhibit electron densities at the BCP characteristic of a
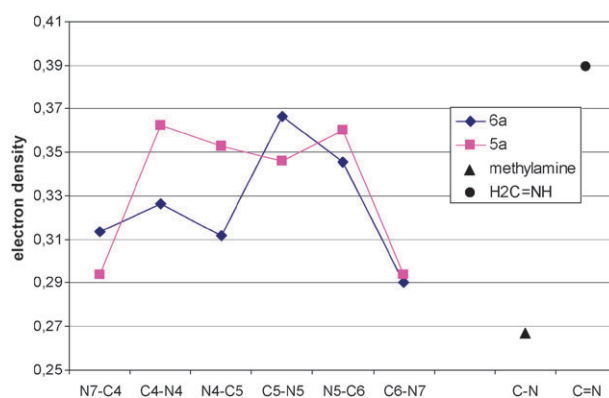
single bond. The protonation at N4 changes this situation. The bonds starting from N4, *i.e.* C4–N4 and N4–C5, are depleted from electron density in **6a** (see Fig. 14 and Table 10). In sharp contrast, bond ellipticity shows only minor differences between **5a** and **6a**. The large heptazine system is able to compensate a single protonation better than the double protonation at the triazine derivative.

All N–H bonds in **2a**, **3a** and **6a** show bond characteristics typically observed for amines or imines (compared with the values from the NH-bond of H$_2$C=NH or methylamine for instance, in Table 10). There are no special electronic features for the iminium character of the NH-bonds in **2a**, **3a** or **6a**, since the positive charge is distributed into the heterocyclic ring systems.

Negative values of the Laplacian of the electron density indicate the presence of mainly covalent bonds.[50] This argument holds for all CN bonds in the s-triazine and s-heptazine rings in Table 10. The positive values of $\nabla^2\rho$ at the BCPs of the PN-bonds are remarkable and deserve further attention. The graphical representation of the Laplacian of the dication of **2a** in Fig. 15 supports the assumption that these bonds are very polar.

The situation is similar in the other four molecules **2b**, **3a**, **5a** and **6a**. P–N bonding in iminophosphoranes has been described previously as highly polar, and it was concluded that the ionic (ylidic) form P$^+$–N$^-$ was much more important than the P=N form.[9,51] Further information can be drawn from the natural charges. The carbon atoms in the ring systems of **2a**, **2b**, **3a**, **5a**, and **6a** are positively charged with values around 0.6, and the nitrogen atoms negatively charged with values around −0.6, which hints towards polar covalent bonds. The PN-bonds in all five molecules reveal a much more pronounced charge difference with charges at N ranging between −0.94 and −1.05 and between 1.53 and 1.92 at P (full data is provided in the ESI†). That means the bonding situation is dominated by the ionic form (P$^+$–N$^-$), and these strong electrostatic interactions are responsible for the short P–N bonding distances.[52] This finding is in accord with an experimental charge density study by Stalke *et al.*, which also revealed predominantly ylidic contributions to a formal P=N double bond.[34] Protonation at the heterocyclic rings has an insignificant influence on the polarity of the PN-bonds.
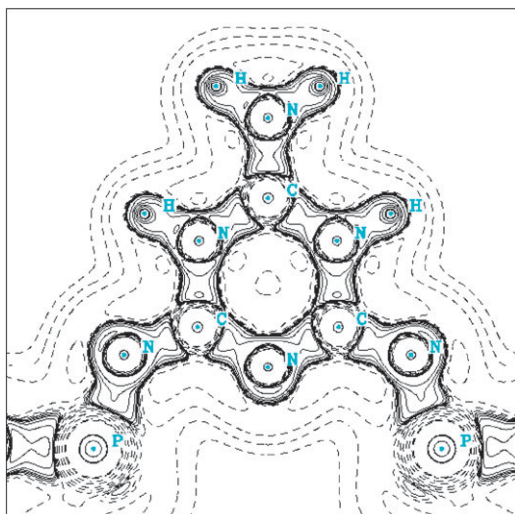
Fig. 15 Laplacian of the electron density of **2a** in the plane of the six-membered ring. Positive values of $\nabla^2\rho$ are drawn with dashed lines and represent regions of charge depletion; negative values are drawn with solid lines and represent regions of charge concentration. Contour values in atomic units are: 0.001, 0.002, 0.004, 0.008, 0.02, 0.04, 0.08, 0.2, 0.4, 0.8, 2, 4, 8, 20, 40, 80, 200, 400, 800.

### Thermogravimetry and flammability test

It has been reported that compounds which contain both phosphorus and nitrogen atoms show a synergetic effect with respect to fire-retardant activity.[7,53] The flame retardancy of this combination proceeds by an intumescent model of action, where the fire-retardant forms char and foam on the surface of a burning substance building up an insulating barrier between the fire and the substrate. Among alternative candidates, intumescent materials have received considerable attention because they provide fire protection with a minimal overall amount of hazardous combustion/pyrolysis products.[54]

Therefore, the fire protection ability of the synthesized compound **7**, which comprises a conjugated carbon–nitrogen–phosphorus system, and at the same time is halogen-free, is of significant interest. Thus, we decided to investigate the thermal decomposition and flame retardancy of **7**. In Fig. 16 the results of thermogravimetric analysis of **7** are shown. Compound **7** is stable up to 140 °C. Between 140 and 240 °C the mass decreases by 4%. At 756 °C the weight loss is 76.6%.

The thermal stability of **7** permits its further examination for flame retardancy in plastics, such as polyamide (PA) and polypropylene (PP). Among the most commonly used flammability tests such as the cone calorimeter test,[55] the "limiting oxygen test" (LOI),[56] and the inflammability test UL 94[57] we have chosen the latter one to estimate the flame retardancy of **7**. Specimen preparation proceeded by mixing **7** with the molten polymer in a 1:4 ratio at 180 °C (PP) and 210 °C (PA) followed by extrusion. Whereas the mixture of **7** with PA polymerized in the extruder, the combination of PP and **7** resulted in specimens suitable for the UL 94 vertical burning test. The results of these flammability test resulted in a "V2 burning class category" for compound **7**, which indicates that a significant fire-retardant effect is observed.
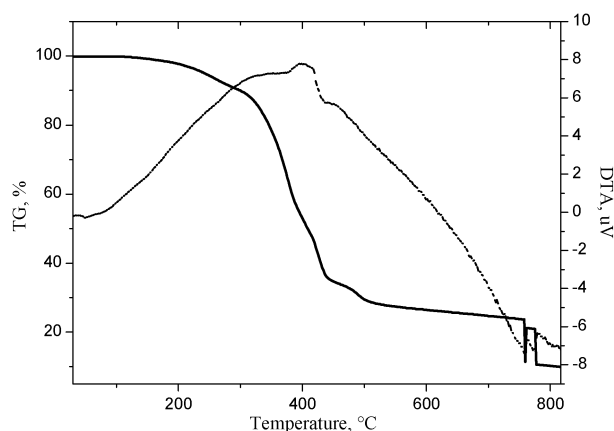


Fig. 16 TG (solid line) and DTA (dashed line) curves of **7**.

### Conclusion

The Kirsanov reaction between melamine and melem with phosphorus pentachloride resulted in symmetrically substituted iminophosphoranes **1** and **5**. In contrast, the use of triphenylphosphine dibromide under similar conditions leads only to partial condensation of the s-triazine core with two phosphinimine groups, accompanied by protonation of the s-triazine ring (compound **2**), whereas in case of the s-heptazine the analogous reaction failed. Since the Kirsanov reaction proceeds by nucleophilic displacement of the halogen from phosphorus by nitrogen atoms, the nucleophilicity of the NH$_2$-groups in the s-heptazine compound melem is significantly decreased as compared to melamine. By deprotonation of **2** with triethylamine only one proton can be removed, yielding monohydrobromide **3**.

Crystal structure analyses of **2**, **3** and **6** clearly indicated a relatively high basicity of the triazine and heptazine N-atoms, which are prevailing for proton attack, in contrast to imine nitrogen atoms. By deprotonation of **2** in solution a proton rearrangement takes place leading to compound **3**. At the same time, the QTAIM analysis shows that the positive charges in **2a** are *not* localized at the nitrogen atoms. Instead, the double protonation leads to a lowering of the bonding degree along the bonds C3–N3 and C1–N2 which is accompanied by a lengthening of these bonds. Single protonation of the triazine ring in **3** also leads to the N1–C3 bond elongation, though not so drastic as in case of **2**. The larger heptazine system proved to have a better ability to cope with the single protonation, than those of s-triazine. Only minor changes in the electron density distribution are observed. Furthermore, compounds **1**, **5** and **6** represent layered structures in the solid state, which are characterised by intermolecular Cl⋯N interactions.

One of the potential applications of s-heptazine-based iminophosphoranes as halogen-free flame-retarding additives was examined by the UL 94 burning test. For this purpose the target compound **7** was obtained from **5** on a large scale by substitution with phenol. The positive result of the testing provides motivation for further investigation in this area.

In summary, the Kirsanov reaction is a simple route to melamine- and melem-derived iminophosphoranes, which

allows production of desired products from commercially available starting materials. The obtained products have good solubility in organic solvents and high reactivity of the phosphinimine groups. Both factors permit further derivatisation of the named materials, making the s-triazine, and particularly the s-heptazine, building blocks readily available for synthetic chemistry.

# Experimental

## General comments

All manipulations were performed in Schlenk-type glassware or in a glove box (MBraun, Germany, $O_2 < 0.1$ ppm, $H_2O < 0.1$ ppm). All solvents were purified and dried according to general procedures. Commercially available chemicals were used in p.a. quality as obtained from the suppliers. Triphenylphosphine dibromide ($Ph_3PBr_2$) was synthesized according to the literature.[20] Melamine, phosphorus pentachloride and anhydrous phenol were purchased from Merck and Fluka. 2,5,8-Triamino-s-heptazine (melem) was synthesized according to a published procedure.[58]

IR spectra were recorded in the range 400–4000 cm$^{-1}$ at room temperature using a Nicolet 380 FT-IR spectrometer. The samples (KBr pellets) were prepared under $N_2$ atmosphere using dry KBr powder.

$^1$H, $^{13}$C and $^{31}$P NMR spectra were recorded on DPX 400 Bruker spectrometer at 300 K. Chemical shifts are reported relative to tetramethylsilane ($^1$H, $^{13}$C NMR) and 85% phosphoric acid ($^{31}$P NMR).

Thermogravimetry measurements were recorded using a TG/DTA thermogravimeter from Seiko Instruments with a heating rate of 5 °C min$^{-1}$, argon flow rate of 300 ml min$^{-1}$, maximum temperature 818 °C.

Elemental analyses were performed with a "vario Micro cube" elemental analyzer (Elementar). Analysis of the chlorine content of product **7** was performed by dissolution in a $Na_2CO_3/K_2CO_3$-melt followed by chloride quantification with ion chromatography (Dionex, ICS-2000, eluent 22 mM KOH, column: AS11_HC, electrical conductivity measurement).

Flammability tests were performed at TITK (Thüringisches Institut für Textil-und-Kunststoff-Forschung e.V.). The vertical burning test for UL 94 classification was carried out on four specimens (90 mm × 13 mm × 2 mm), prepared from polypropylene and compound **7** in a 4 : 1 ratio by extrusion at 180 °C.

**Single-crystal X-ray diffraction analyses.** Diffraction data were collected on a BRUKER NONIUS X8 APEX2 CCD diffractometer using Mo-Kα radiation. The structures were solved with direct methods and refined with full-matrix least-squares methods on $F^2$ [with the software SHELXS-97 and SHELXL-97, G. M. Sheldrick, Universität Göttingen (1986–1997)]. All non-hydrogen atoms were anisotropically refined. Carbon-bonded hydrogen atoms were placed in idealized positions and isotropically refined (riding model). N-bound hydrogen atoms were found by analysis of the residual electron density and refined without bond length restraints. Data of structure determination and refinement for the herein presented crystal structures are summarized in the ESI.†

**Quantum chemical calculations.** The quantum chemical calculations were carried out using the GAUSSIAN 03 series of programs.[59] Geometries were fully optimized at the density functional theory level (DFT), using Becke's three-parameter hybrid exchange functional and the correlation functional of Lee, Yang and Parr (B3LYP)[60,61] in combination with the 6-31G(d,p) basis set.[62,63] The optimized geometries were verified as local minima on the potential energy surface by calculating the Hessian matrices. The QTAIM analyses[47] have been performed at the same level of theory with the optimized geometries. The wavefunction files for the QTAIM analysis were generated in Cartesian coordinates with a basis set containing 6d functions (option "6D 10F" in Gaussian03). The electron density topology was analyzed using the programs AIM2000[64] and Xaim.[65] The natural charges were obtained from calculations with NBO 5.0.[66] Relative energies of **3a–d** are calculated from the electronic energies including zero-point correction from optimized geometries at the B3LYP/6-31G(d,p) level.

**Preparation of tris(trichlorophosphinimino)-s-triazine (1).** 10 g (0.08 mol) of melamine $C_3N_6H_6$ and 49.5 g (0.24 mol) of $PCl_5$ were suspended in 260 ml of dry 1,2-dichlorobenzene. The reaction mixture was heated to reflux, whereupon the starting materials completely dissolved and the liberation of HCl gas commenced. After 10 h under reflux, when no further liberation of HCl gas was observed, the clear yellow reaction solution was cooled down to room temperature, and its volume was reduced to 100 ml. By cooling the reaction mixture down to 0 °C white crystals appeared. Yield: 38.6 g (90.7%). IR (KBr): 1580 (vs), 1460 (s), 1380 (w), 1250 (s), 1100 (s), 1040 (w), 874 (m), 822 (m), 586 (s), 559 (s), 521 (m), 430 (w). NMR (1,2-dichlorobenzene, ppm, Hz): $^{31}$P: 7.1. $^{13}$C: 168.7, $^2J_{P-C} = 13.78$.

**Preparation of 2-amino-4,6-bis(triphenylphosphinimino)-s-triazine dihydrobromide (2·$C_6H_4Cl_2$).** In a 250 ml round-bottomed Schlenk-flask 1.37 g (0.01 mol) of melamine $C_3N_6H_6$ and 12.72 g (0.03 mol) of $Ph_3PBr_2$ were suspended in 80 ml of dry 1,2-dichlorobenzene. The suspension was stirred under reflux for 30 h; thereafter the unreacted melamine was filtered off. The brown solution was cooled down to 0 °C until white crystals appeared. Yield: 7.5 g (86%). IR: 3090 (m), 3060 (m), 2960 (m), 2930 (s), 2860 (m), 2790 (w), 1700 (s), 1615 (s), 1610 (s), 1520 (s), 1440 (m), 1390 (vs), 1320 (w), 1190 (w), 1120 (s), 1030 (w), 997 (w), 950 (m), 876 (m), 766 (m), 724 (s), 687 (s), 669 (m), 636 (w), 519 (s). NMR (1,2-dichloroethane, ppm, Hz): $^{31}$P: 18.8. $^{13}$C: 132.8, $^4J_{C-P} = 1.2$, p-C, P–$C_6H_5$; 131.8, $^2J_{C-P} = 8.3$, o-C, P–$C_6H_5$; 128.5, $^3J_{C-P} = 13.2$, m-C, P–$C_6H_5$; 124.2, $^1J_{C-P} = 101.8$, i-C, P–$C_6H_5$. $^1$H: 8.7, N$_{triaz}$–H, 6.9–6.5, m, C–H (Ph), 3.3 NH$_2$.

**Preparation of 2-amino-4,6-bis(triphenylphosphinimino)-s-triazine hydrobromide (3·Et$_3$NHBr·1.5$C_6H_4Cl_2$).** To a solution of 2·$C_6H_4Cl_2$ (1 g, 1.04 mmol) in 30 ml of dichlorobenzene, an excess of triethylamine (1.2 ml, 8.7 mmol) was added dropwise. The light-yellow suspension was refluxed for 10 h and the white precipitate was filtered off. The single crystals of 3·Et$_3$NHBr·1.5$C_6H_4Cl_2$ were obtained by recrystallisation of the obtained precipitate from o-dichlorobenzene. Yield: 0.63 g

of **3**·Et$_3$NHBr·1.5C$_6$H$_4$Cl$_2$; 0.45 g 53.5% of **3**. IR: 3300 (w), 3140 (m), 3060 (m), 2980 (m), 2940 (m), 2740 (w), 2680 (m), 2490 (w), 1640 (m), 1580 (s), 1550 (s), 1480 (m), 1440 (s), 1330 (s), 1290 (m), 1190 (w), 1110 (s), 1040 (m), 867 (m), 794 (m), 725 (s), 693 (s), 666 (w), 532 (s). NMR (1,2-dichloroethane, ppm, Hz) [31]P: 21.1. [13]C: 132.2, [2]$J_{C-P}$ = 10.7, *o*-C, P–C$_6$H$_5$; 131.9, [4]$J_{C-P}$ = 2.8, *p*-C, P–C$_6$H$_5$; 127.9, [3]$J_{C-P}$ = 12.5, *m*-C, P–C$_6$H$_5$; 125.3, [1]$J_{C-P}$ = 102.7, *i*-C, P–C$_6$H$_5$. [1]H: 6.9, N$_{triaz}$–H, 6.8–6.5, m, C–H (Ph), 2.5 NH$_2$. Elemental analyses (%), found (calcd.): C 55.94 (57.39), N 9.13 (8.68), H 4.67 (4.90).

**Preparation of triphenylphosphine chloride–bromide (4·C$_2$H$_4$Cl$_2$).** 1 g (4.6 mmol) of melem was suspended in 80 ml of 1,2-dichloroethane. By accident, a very large amount of Ph$_3$PBr$_2$ (17.4 g, 41 mmol) was added to the suspension. The mixture was stirred under reflux for 5 h, followed by 10 h at room temperature. The reaction flask was cooled down to 0 °C, and after 20 h at this temperature a big cubic-like crystal had formed. ^{31}P-NMR (1,2-dichloroethane, ppm): 58.2.

**Preparation of tris(trichlorophosphinimino)-s-heptazine (5·C$_6$H$_4$Cl$_2$).** To the mixture of 10 g (0.046 mol) of melem, 31 g (0.15 mol) of PCl$_5$ and 350 ml of dry 1,2-dichlorobenzene were added. The obtained suspension was stirred under reflux for 45 h. The course of the reaction was monitored by measuring the volume of liberated HCl gas. Thereafter the unreacted melem and PCl$_5$ were filtered off and the yellowish filtrate was collected. The solvent was removed in vacuum and the solid residue dried in vacuum at 70–80 °C. Single crystals of **5**·C$_6$H$_4$Cl$_2$ suitable for X-ray structure analysis were obtained by cooling a solution in *o*-dichlorobenzene down to 0 °C. Yield: 26 g, 91%. M. p. = 148–153 °C (from *o*-C$_6$H$_4$Cl$_2$). IR: 1630 (s); 1539 (m); 1456 (vs); 1414 (vs); 1355 (s); 1304 (s); 1259 (s); 1184 (m); 1126 (m); 1079 (m); 1034 (m); 945 (m); 905 (m); 819 (m); 808 (m); 746 (m); 640 (m); 623 (m); 538 (s); 486 (m); 452 (m). NMR (1,2-dichloroethane, ppm): ^{31}P NMR: 19.2. ^{13}C-NMR: 167.5, 156.5.

**Preparation of tris(trichlorophosphinimino)-s-heptazine hydrochloride (6·C$_2$H$_4$Cl$_2$).** Compound **6**·C$_2$H$_4$Cl$_2$ was obtained by recrystallization of **5** from 1,2-dichloroethane. IR: 3100 (broad, m), 1674 (s), 1625 (s), 1527 (m), 1418 (vs), 1372 (vs), 1267 (s), 1215 (m), 1069 (s), 1016 (m), 809 (s), 731 (m), 639 (s), 580 (s), 486 (m), 442 (m). NMR (1,2-dichloroethane, ppm): ^{31}P NMR: 22.3. ^{13}C-NMR: 167.5, 156.6.

**Preparation of tris(2,5,8-triphenoxyphosphinimino)-s-heptazine (7).** At 0 °C, a solution of anhydrous phenol (14 g, 0.15 mol) in 30 ml of 1,2-dichloroethane was slowly added to a solution of 10 g (0.016 mol) of **5** in 80 ml of 1,2-dichloroethane. The solution was stirred for 1 h at this temperature and then slowly warmed to room temperature. During addition and further stirring liberation of gaseous HCl was observed. The reaction mixture was stirred for 5 h in a very slow stream of argon; thereafter the solvent and unreacted phenol were removed in vacuum. The product was isolated as a yellowish resin-like solid. Yield: 16 g, 87.5%, IR: 3060 (m), 1631 (s), 1587 (s), 1538 (m), 1487 (s), 1413 (vs), 1307 (m), 1204 (s), 1187 (m), 1158 (s), 1087 (s), 1025 (m), 1013 (m), 974 (s), 818 (w), 809 (m), 775 (s), 752 (s), 686 (s), 650 (w), 617 (m), 575 (m), 493 (m). NMR (1,2-dichloroethane, ppm, Hz):

^{31}P-NMR: −5.9. ^{13}C-NMR: 150.06, [2]$J_{C-P}$: 7.04, *i*-C; 129.00, *m*-C; 124.49, *p*-C; 119.21, [3]$J_{C-P}$: 4.93, *o*-C. [1]H: m, 6.7–6.5. Elemental analyses (%), found (calcd.) C 62.31 (63.05), N 12.20 (12.60), H 3.93 (3.97), Cl 0.0 (0.0).

## References and notes

1 Tri-*s*-triazine is also known as *sym*-heptazine, 1,3,4,6,7,9,9b-heptaaza-phenallene, 1,3,4,6,7,9-hexaazacyclo[3.3.3]azine or cyamelurine.
2 (*a*) M. L. Cohen, *Phys. Rev. B: Condens. Matter*, 1985, **32**, 7988; (*b*) T. Malkow, *Mater. Sci. Eng., A*, 2000, **292**, 112; (*c*) E. Kroke and M. Schwarz, *Coord. Chem. Rev.*, 2004, **248**, 493; (*d*) B. V. Lotsch, M. Döblinger, J. Sehnert, L. Seyfarth, J. Senker, O. Oeckler and W. Schnick, *Chem.–Eur. J.*, 2007, **13**, 4969; (*e*) Y. Zhao, Zh. Liu, W. Chu, Li Song, Z. Zhang, D. Yu, Y. Tian, S. Xie and L. Sun, *Adv. Mater.*, 2008, **20**, 1777; (*f*) M. J. Bojdys, J.-O. Müller, M. Antonietti and A. Thomas, *Chem.–Eur. J.*, 2008, **14**, 8177.
3 (*a*) K. Mori, *Hyomen Gijutsu*, 2000, **51**, 276; (*b*) N. Ohta, *J. Photochem. Photobiol., C*, 2000, **1**, 195; (*c*) G. Blotny, *Tetrahedron*, 2006, **62**, 9507; (*d*) J. Yoo, P. Jadhav and E. Kim, *Mol. Cryst. Liq. Cryst.*, 2008, **491**, 114.
4 (*a*) R. Riedel, E. Horvath-Bordon, S. Nahar-Borchert and E. Kroke, *Key Eng. Mater* (Advanced Ceramics and Composites), 2003, vol. 247, p. 121; (*b*) B. Juergens, E. Irran, J. Senker, P. Kroll, H. Mueller and W. Schnick, *J. Am. Chem. Soc.*, 2003, **125**, 10288; (*c*) N. E. A. El-Gamel, M. Schwarz, E. Brendler and E. Kroke, *Chem. Commun.*, 2006, 4741; (*d*) A. Thomas, A. Fischer, F. Goettmann, M. Antonietti, J.-O. Müller, R. Schlögl and J. M. Carlsson, *J. Mater. Chem.*, 2008, **18**, 4893; (*e*) J. R. Holst and E. G. Gillan, *J. Am. Chem. Soc.*, 2008, **130**, 7373.
5 (*a*) I. Hechenbleikner, *US Pat*. US 2832745, 1958; (*b*) Sh. Akitaya, T. Fukazawa and N. Tabata, *Jpn. Pat*. JP 04142348, 1992; (*c*) T. Koizumi, Y. Nakamura and M. Yamaguchi, *Jpn. Pat* JP 2005232310, 2005; (*d*) H. Sakamoto, T. Noda and Y. Nakada, *Jpn. Pat*. JP 2007161774, 2007.
6 (*a*) J. Murphy, *Plast. Addit. Compd.*, 2001, **3**, 16; (*b*) A. Mukherjee, *Plastics Eng.*, 2001, **57**, 42; (*c*) C. Boelens and R. Grabner, *Recent Advances in Flame Retardancy of Polymeric Materials*, 1999, **10**, 184; (*d*) A. König, U. Fehrenbacher, E. Kroke and T. Hirth, *J. Cell. Plast.*, 2008, **44**, 469.
7 T.-S. Leu and C.-S. Wang, *J. Appl. Polym. Sci.*, 2004, **92**, 410.
8 See *e.g.* (*a*) A. Y. Garner, *US Pat*. US 4020224, 1977; (*b*) Fr. Demande and A. G. Ciba-Geigy, *Fr. Pat*. FR 2202132 19740503, 1974; (*c*) R. Begrich and A. G. Ciba-Geigy, *Ger. Pat*. DE 2331518, 1974; (*d*) M. N. Kolganova, F. A. Levites, N. M. Moskovskaya, V. D. Korzhov, A. S. Samovolov, V. P. Salyuk, V. A. Kostenko, A. L. Leiviman and I. A. Grishina, *USSR Pat*. SU 902450, 1986; (*e*) J. S. Leake, *World Pat*. WO 9312173, 1993; (*f*) T. Gmeiner, E. Kroke and M. Schwarz, *World Pat*. WO 2006034784, 2006.
9 A. W. Johnson, W. C. Kaska, K. A. O. Starzewski and D. A. Dixon, *Ylides and Imines of Phosphorus*, Wiley, New York, 1993.
10 H. Staudinger and J. Meyer, *Helv. Chim. Acta*, 1919, **2**, 635.
11 A. V. Kirsanov, *Isv. Akad. Nauk SSSR*, 1950, 426; A. V. Kirsanov, *Chem. Abstr.*, 1951, **45**, 1503; A. V. Kirsanov, *Zh. Obshch. Khim.*, 1952, **22**, 269; A. V. Kirsanov, *Chem. Abstr.*, 1952, **46**, 11135.
12 W. Kesting, *J. Prakt. Chem.*, 1923, **105**, 242.

13 (a) E. Keßenich, T. M. Klapötke, J. Knizek, H. Nöth and A. Schulz, *Eur. J. Inorg. Chem.*, 1998, 2013; (b) E. Keßenich, K. Polborn and A. Schulz, *Inorg. Chem.*, 2001, **40**, 1102.

14 (a) T. Gmeiner, *Diploma Thesis*, University of Konstanz, 2005; (b) T. Saplinova, V. Bakumov, T. Gmeiner, J. Wagler, M. Schwarz and E. Kroke, *Z. Anorg. Allg. Chem.*, 2009, **635**, 2480.

15 (a) E. Ott and E. Ohse, *Ber. Dtsch. Chem. Ges.*, 1921, **54**, 179; (b) E. Kroke, M. Schwarz, V. Buschmann, G. Miehe, H. Fueß and R. Riedel, *Adv. Mater.*, 1999, **11**, 158; (c) E. G. Gillan, *Chem. Mater.*, 2000, **12**, 3906; (d) T. M. Klapoetke and C. M. Rienacker, *Propellants, Explos., Pyrotech.*, 2001, **26**, 43.

16 (a) D. R. Miller, D. C. Swenson and E. G. Gillan, *J. Am. Chem. Soc.*, 2004, **126**, 5372; (b) E. Kroke, *Habilitation*, TU Darmstadt, 2004; (c) A. Hammerl, T. M. Klapoetke and R. Rocha, *Eur. J. Inorg. Chem.*, 2006, 2210; (d) D. R. Miller, J. R. Holst and E. G. Gillan, *Inorg. Chem.*, 2007, **46**, 2767.

17 G. Gotsman and M. Schwarzmann, *Justus Liebigs Ann. Chem.*, 1969, **729**, 106.

18 (a) L. A. Lazukina, N. G. Kotlyar, V. P. Kukhar and S. N. Solodushenkov, *Zhurnal Obshchei Kimii*, 1971, **41**, 2386; (b) V. Ya. Semenii, A. P. Boiko, G. F. Solodushchenko, N. A. Kirsanova and V. P. Kukhar, *Zhurnal Obshchei Khimii*, 1974, **44**, 1251; (c) F. Belaj, *Phosphorus, Sulfur Silicon Relat. Elem.*, 1996, **109–110**, 71.

19 G. I. Derkach, M. I. Bukovskii, S. N. Solodushenkov and A. I. Mosiichuk, *Khim. Org. Soedin. Fosfora, Akad. Nauk SSSR, Otd. Obshch. Tekh. Khim.*, 1967, 89.

20 F. P. Cossio, I. Ganboa and C. Palomo, *Tetrahedron Lett.*, 1985, **26**, 3041.

21 M. R. Churchill and S. A. Julis, *Inorg. Chem.*, 1978, **17**, 3011.

22 J. C. Previdi and R. A. Krause, *Inorg. Nucl. Chem. Lett.*, 1971, **7**, 647.

23 (a) P. Coppens and A. Vos, *Acta Crystallogr., Sect. B: Struct. Crystallogr.Cryst. Chem.*, 1971, **27**, 146; (b) A. Sattler and W. Schnick, *Z. Anorg. Allg. Chem.*, 2006, **632**, 1518.

24 S. J. Maginn, R. G. Compton, M. S. Harding, C. M. Brennan and R. Docherty, *Tetrahedron Lett.*, 1993, **34**, 4349.

25 N. E. A. El-Gamel, J. Brand and E. Kroke, *J. Coord. Chem.*, 2009, **62**, 1278–1284.

26 (a) G. R. Desiraju, *Crystal Engineering: The Design of Organic Solids*, Elsevier, 1989; (b) H. A. Bent, *Chem. Rev.*, 1968, **68**, 587.

27 R. A. Pascal Jr. and D. M. Ho, *Tetrahedron Lett.*, 1992, **33**, 4707.

28 S. Tragl and H.-J. Meyer, *Z. Anorg. Allg. Chem.*, 2005, **631**, 2300.

29 (a) E. Kroke, M. Schwarz, E. Horath-Bordon, P. Kroll, B. Noll and A. D. Norman, *New J. Chem.*, 2002, **26**, 508; (b) E. Bordon, E. Kroke, I. Svoboda, H. Fueß, R. Riedel, N. Sharma and A. K. Cheetham, *Dalton Trans.*, 2004, 3900; (c) E. Horvath-Bordon, E. Kroke, I. Svoboda, H. Fueß and R. Riedel, *New J. Chem.*, 2005, **29**, 693; (d) M. R. Schwarz, H. Ehrenberg, M. A. Kloc and E. Kroke, *Heterocycles*, 2006, **68**, 2499; (e) N. E. A. El-Gamel, J. Wagler and E. Kroke, *J. Mol. Struct.*, 2008, **888**, 204; (f) C. Clauss, J. Wagler, M. Schwarz, A. Schwarzer and E. Kroke, *Z. Anorg. Allg. Chem.*, 2010, **636**, 196.

30 A. Bondi, *J. Phys. Chem.*, 1964, **68**, 441.

31 J. N. Varghese, A. M. O'Connell and E. N. Maslen, *Acta Crystallogr., Sect. B: Struct. Crystallogr. Cryst. Chem.*, 1977, **33**, 2102.

32 (a) E. Irran, B. Jürgens and W. Schnick, *Solid State Sci.*, 2002, **4**, 1305; (b) B. Jürgens, H. A. Höppe and W. Schnick, *Z. Anorg. Allg. Chem.*, 2004, **630**, 35.

33 P. Rademacher, *Strukturen organischer Moleküle*, Physikalische Organische Chemie, Vol. 2, VCH, Weincheim, New York, 1987.

34 N. Kocher, D. Leusser, A. Murso and D. Stalke, *Chem.–Eur. J.*, 2004, **10**, 3622.

35 J. Kaiser, H. Hartung and R. Richter, *Z. Anorg. Allg. Chem.*, 1980, **469**, 188.

36 (a) J. Janczak and G. J. Perpetuo, *Acta Crystallogr., Sect. C: Cryst. Struct. Commun.*, 2001, **57**, 1120; (b) K. Wijaya, O. Moers, D. Henschel, A. Blaschette and P. G. Jones, *Z. Naturforsch. B*, 2004, **59**, 747; (c) P. Nockemann and G. Meyer, *Z. Anorg. Allg. Chem.*, 2004, **630**, 2571; (d) J. Zhang, Y. Kang, Yi-H. Wen, Zh.-Ji.. Li, Ye-Yan Qin and Y.-G. Yao, *Acta Crystallogr., Sect. E: Struct. Rep. Online*, 2004, **60**, o462; (e) G. J. Perpetuo, M. A. Ribeiro and J. Janczak, *Acta Crystallogr., Sect. E: Struct. Rep. Online*, 2005, **61**, o1818.

37 F. H. Allen, O. Kennard, D. G. Watson, L. Brammer, A. G. Orpen and R. Taylor, *J. Chem. Soc., Perkin Trans. 2*, 1987, S1.

38 A. I. Finkel'shtein and N. V. Spiridonova, *Russ. Chem. Rev.*, 1964, **33**, 400.

39 So far, only very few examples concerning reactivity of the $NH_2$-groups in melem have been reported: (a) R. I. Spasskaya, A. I. Finkel'stein, E. N. Zil'berman and V. A. Gal'perin, *Zhurnal Obschchei Khimii*, 1976, **46**, 1423; (b) A. S. Gordetsov, Yu. I. Dergunov and N. K. Gavrilova, *Khimiya Elementoorgan. Soedin.*, 1980, **8**, 59.

40 A. Sattler, L. Seyfarth, J. Senker and W. Schnick, *Z. Anorg. Allg. Chem.*, 2005, **631**, 2545.

41 N. S. Kumar, K. P. Kumar, K. V. P. P. Kumar, P. Kommana, J. J. Vittal and K. C. K. Swamy, *J. Org. Chem.*, 2004, **69**, 1880.

42 (a) N. E. A. El-Gamel, L. Seyfarth, J. Wagler, H. Ehrenberg, M. Schwarz, J. Senker and E. Kroke, *Chem.–Eur. J.*, 2007, **13**, 1158; (b) A. Sattler and W. Schnick, *Z. Anorg. Allg. Chem.*, 2008, **634**, 457.

43 W. Zheng, N.-B. Wong and A. Tian, *J. Phys. Chem. A*, 2005, **109**, 1926.

44 R. J. Boyd, S. C. Choi and C. C. Hale, *Chem. Phys. Lett.*, 1984, **112**, 136.

45 W. Zheng, N.-B. Wong, W.-K. Li and A. Tian, *J. Phys. Chem. A*, 2004, **108**, 11721.

46 W. Zheng, N.-B. Wong, Ge Zhou, X. Liang, J. Lic and A. Tian, *New J. Chem.*, 2004, **28**, 275.

47 R. F. W. Bader, *Atoms in Molecules*, Clarendon Press, Oxford, 1994.

48 R. J. Gillespie, *J. Chem. Educ.*, 2001, **78**, 1688.

49 R. A. Gillespie and P. L. A. Popelier, *Chemical Bonding and Molecular Geometry*, Oxford University Press, New York, 2001.

50 R. F. W. Bader and H. Essén, *J. Chem. Phys.*, 1984, **80**, 1943.

51 J. Koketsu, Y. Ninomiya, Y. Suzuki and N. Koga, *Inorg. Chem.*, 1997, **36**, 694.

52 H. Folkerts, W. Hiller, M. Herker, S. F. Vyboishchikov, G. Frenking and K. Dehnicke, *Angew. Chem., Int. Ed. Engl.*, 1995, **34**, 1362.

53 M. Lewin and E. D. Weil, 'Mechanisms and modes of action in flame retardancy of polymers', in *Fire retardant materials*, ed. A. R. Horrocks and D. Price, Woodhead Publishing Ltd and CRC Press LLC, 2001, ch. 2.

54 Ch. E. Anderson, Jr., J. Dziuk, Jr., W. A. Mallow and J. Buckmaster, *J. Fire Sci.*, 1985, **3**, 161.

55 ISO 5660-1: 1993, *Fire tests – Reaction to Fire – Part 1: Rate of Heat Release from Building Products (Cone Calorimeter Method)*, International Standards Organisation, Geneva, Switzerland, 1993.

56 Deutsches Institut für Normung e.V. DIN EN ISO 4589-2, Beuth Verlag, Berlin, 1999.

57 Deutsches Institut für Normung e.V. DIN IEC 60695-11-10, Beuth Verlag, Berlin, 1999.

58 B. V. Lotsch and W. Schnick, *Chem.–Eur. J.*, 2007, **13**, 4956.

59 M. J. Frisch, G. W. Trucks, H. B. Schlegel, G. E. Scuseria, M. A. Robb, J. R. Cheeseman, J. A. Montgomery Jr., T. Vreven, K. N. Kudin, J. C. Burant, J. M. Millam, S. S. Iyengar, J. Tomasi, V. Barone, B. Mennucci, M. Cossi, G. Scalmani, N. Rega, G. A. Petersson, H. Nakatsuji, M. Hada, M. Ehara, K. Toyota, R. Fukuda, J. Hasegawa, M. Ishida, T. Nakajima, Y. Honda, O. Kitao, H. Nakai, M. Klene, X. Li, J. E. Knox, H. P. Hratchian, J. B. Cross, C. Adamo, J. Jaramillo, R. Gomperts, R. E. Stratmann, O. Yazyev, A. J. Austin, R. Cammi, C. Pomelli, J. W. Ochterski, P. Y. Ayala, K. Morokuma, G. A. Voth, P. Salvador, J. J. Dannenberg, V. G. Zakrzewski, S. Dapprich, A. D. Daniels, M. C. Strain, O. Farkas, D. K. Malick, A. D. Rabuck, K. Raghavachari, J. B. Foresman, J. V. Ortiz, Q. Cui, A. G. Baboul, S. Clifford, J. Cioslowski, B. B. Stefanov, G. Liu, A. Liashenko, P. Piskorz, I. Komaromi, R. L. Martin, D. J. Fox, T. Keith, M. A. Al-Laham, C. Y. Peng, A. Nanayakkara, M. Challacombe, P. M. W. Gill, B. Johnson, W. Chen, M. W. Wong, C. Gonzalez and J. A. Pople, *GAUSSIAN 03, Revision C.02*, Gaussian, Inc., Wallingford CT, 2004.

60 A. D. Becke, *J. Chem. Phys.*, 1993, **98**, 5648.

61 P. J. Stevens, F. J. Devlin, C. F. Chablowski and M. J. Frisch, *J. Phys. Chem.*, 1994, **98**, 11623.

62 P. C. Hariharan and J. A. Pople, *Theor. Chim. Acta*, 1973, **28**, 213.

63 M. M. Francl, W. J. Pietro, W. J. Hehre, J. S. Binkley, M. S. Gordon, D. J. DeFrees and J. A. Pople, *J. Chem. Phys.*, 1982, **77**, 3654.

64 F. Biegler-König, J. Schönbohm and D. Bayles, AIM2000-A Program to Analyze and Visualize Atoms in Molecules, *J. Comput. Chem.*, 2001, **22**, 545.

65 *Xaim*, developed by Jose Carlos Ortiz and Carles Bo, Universitat Rovira i Virgili, Tarragona, Spain.

66 E. D. Glendening, J. K. Badenhoop, A. E. Reed, J. E. Carpenter, J. A. Bohmann, C. M. Morales and F. Weinhold, *NBO 5.0*, Theoretical Chemistry Institute, University of Wisconsin, Madison, 2001.